

Article

**Methyl 3-((6-methoxy-1,4-dihydroindeno[1,2-c]pyrazol-3-yl)amino) benzoate (GN39482) as a Tubulin Polymerization Inhibitor Identified by MorphoBase and ChemProteoBase Profiling Methods**

Hidemitsu Minegishi, Yushi Futamura, Shinji Fukashiro, Makoto Muroi, Makoto Kawatani, Hiroyuki Osada, and Hiroyuki Nakamura

*J. Med. Chem.*, **Just Accepted Manuscript** • Publication Date (Web): 04 May 2015

Downloaded from <http://pubs.acs.org> on May 4, 2015

**Just Accepted**

"Just Accepted" manuscripts have been peer-reviewed and accepted for publication. They are posted online prior to technical editing, formatting for publication and author proofing. The American Chemical Society provides "Just Accepted" as a free service to the research community to expedite the dissemination of scientific material as soon as possible after acceptance. "Just Accepted" manuscripts appear in full in PDF format accompanied by an HTML abstract. "Just Accepted" manuscripts have been fully peer reviewed, but should not be considered the official version of record. They are accessible to all readers and citable by the Digital Object Identifier (DOI®). "Just Accepted" is an optional service offered to authors. Therefore, the "Just Accepted" Web site may not include all articles that will be published in the journal. After a manuscript is technically edited and formatted, it will be removed from the "Just Accepted" Web site and published as an ASAP article. Note that technical editing may introduce minor changes to the manuscript text and/or graphics which could affect content, and all legal disclaimers and ethical guidelines that apply to the journal pertain. ACS cannot be held responsible for errors or consequences arising from the use of information contained in these "Just Accepted" manuscripts.



**ACS Publications**  
High quality. High impact.

**Methyl 3-((6-methoxy-1,4-dihydroindeno[1,2-c]pyrazol-3-yl)amino) benzoate (GN39482) as a Tubulin Polymerization Inhibitor Identified by MorphoBase and ChemProteoBase Profiling Methods**

Hidemitsu Minegishi,<sup>1,2)</sup> Yushi Futamura,<sup>3)</sup> Shinji Fukashiro,<sup>2)</sup> Makoto Muroi,<sup>3)</sup> Makoto Kawatani,<sup>3)</sup> Hiroyuki Osada,<sup>3)</sup> and Hiroyuki Nakamura<sup>\*,1)</sup>

- 1) Chemical Resources Laboratory, Tokyo Institute of Technology, Nagatsuta-cho, Midori-ku, Yokohama 226-8503, Japan
- 2) Department of Life Science, Faculty of Science, Gakushuin University, Mejiro, Toshima-ku, Tokyo 171-8588, Japan
- 3) Chemical Biology Research Group, RIKEN Center for Sustainable Resource Center, Hirosawa, Wako, Saitama 351-0198, Japan

**Abstract**

A series of indenopyrazoles was synthesized from the corresponding indanones and phenyl isothiocyanates in two steps. Among the compounds synthesized, methyl 3-((6-methoxy-1,4-dihydroindeno[1,2-c]pyrazol-3-yl)amino)benzoate **6m** (GN39482) was found to possess a promising antiproliferative activity toward human cancer cells without affecting any anti-microbial and anti-malarial activities at 100 nM. Both a methoxy group at R<sup>1</sup> position and a methoxycarbonyl group at R<sup>2</sup> position of the anilinoquinazoline framework are essential for the high cell growth inhibition. Both MorphoBase and ChemProteoBase profiling analyses suggested that compound **6m** was classified as a tubulin inhibitor. Indeed, compound **6m** inhibited the acetylated tubulin accumulation and the microtubule formation and induced G2/M cell cycle arrest in HeLa cells, revealing that a promising antiproliferative activity of compound **6m** toward human cancer cells is probably caused by the tubulin polymerization inhibition.

**Keywords**

Indenopyrazole, antiproliferative activity, tubulin polymerization inhibitor, MorphoBase profiling analysis, ChemProteoBase profiling analysis

## Introduction

Indenopyrazole, a novel pseudoazulenic system containing two fused five-membered rings, was first synthesized by Boyd in 1965.<sup>1</sup> Although indenopyrazoles were reported by Lemke and coworkers as potential antipsychotic agents in 1978,<sup>2</sup> other biological activities have not been reported until 1998.<sup>3</sup> Nugiel and coworkers reported indenopyrazoles as cyclin dependent kinase (CDK) inhibitors. After their finding, various indenopyrazole-based CDK inhibitors have been reported.<sup>4, 5</sup> Galemme and coworkers reported platelet-derived growth factor receptor (PDGFR) tyrosine kinase inhibitors,<sup>6</sup> and Tao and coworkers reported checkpoint kinase 1 (Chk1) inhibitors.<sup>7, 8</sup> We also found indenopyrazole-containing inhibitions of epidermal growth factor receptor (EGFR) and vascular endothelial growth factor receptor (VEGFR)-2 tyrosine kinases by *in silico* high-through-put screening (Figure 1).<sup>9</sup> Thus, indenopyrazole has been paid attention as one of the attractive frameworks for development of kinase inhibitors<sup>10</sup> in medicinal chemistry.

Recently much attention has been focused on a hypoxia inducible factor (HIF)-1 inhibitor as a target for anticancer agents because HIF-1 is a transcription factor that controls the expression on genes such as vascular endothelial growth factor (VEGF), erythropoietin (EPO) and insulin like growth factor.<sup>11-13</sup> VEGF and EPO are key factors in tumor growth and pathological angiogenesis. The overexpression of HIF-1 $\alpha$  has been observed in various cancers,<sup>14, 15</sup> including brain, breast, cervical, esophageal, and ovarian cancers correlated with treatment failure and mortality, as a result

of intratumoral hypoxia and genetic alterations affecting key oncogenes and tumor suppressor genes. Therefore, drugs targeting HIF-1 could represent a novel approach to cancer therapy.<sup>16-21</sup> Recently, we reported indenopyrazole **1** (GN44028) as a new HIF-1 inhibitor.<sup>22</sup> In the structure activity relationship (SAR) study based on **1**, indenopyrazole **2** was found to possess unexpectedly high cell growth inhibition toward several cancer cell lines.

(Figure 1)

In this paper, we performed the further SAR study based on cytotoxic compound **2**, and discovered more potent cell growth inhibitors than **2**. Furthermore, we clarified that their promising antiproliferative activity has been caused by inhibiting tubulin polymerization using MorphoBase<sup>23</sup>,<sup>24</sup> and ChemProteoBase<sup>25, 26</sup> profiling methods.

## Results and Discussion

### Chemistry

The synthesis of phenyl isothiocyanates is shown in Scheme 1. Anilines **3a-d**, which were prepared from corresponding 2- or 3-hydroxyl anilines and 3-aminobenzoic acid, and aniline **3e** were treated with phenyl chlorothionoformate in THF to give thiocarbamate intermediates, which reacted with

triethylamine (TEA) and  $\text{Cl}_3\text{SiH}$  to afford phenyl isothiocyanates **4a-e** in high yields.<sup>27</sup>

(Scheme 1)

Scheme 2 shows the formation of indenopyrazoles from the corresponding indanones **5a-c** and phenyl isothiocyanates **4a-j** including commercially available starting materials (**5c** and **4f-j**).

Indanones **5a** and **5b** were prepared from 5-hydroxylindanone with TBS or ethyl protections, respectively. Deprotonation of  $\alpha$ -proton of carbonyls in indanones **5a-c** was carried out using lithium hexamethyldisilazide (LiHMDS) and the resulting enolates reacted with phenyl isothiocyanates **4** to give the thioamide intermediates, that underwent condensation with hydrazine monohydrate to form indenopyrazoles **6** in moderate yields (37-60%). Deprotection of a TBS group in **6b**, **6d** and **6f** was carried out by treatment with TBAF in THF to give indenopyrazoles **6l-m** in moderate to high yields. Methyl ester **6m** was hydrolyzed using LiOH to give indenopyrazole **6n** in 76% yield (Scheme 2).

(Scheme 2)

## Biology

Synthesized indenopyrazoles **6a**, **6c**, **6e**, **6g-q** were tested for antiproliferative activity toward three

human cancer cell lines, HeLa (human cervical carcinoma), PC3 (human prostate cancer) and HCT116 (human colon cancer), and a normal cell line, HEK293 (human embryonic kidney) using MTT assay. We first examined the effect of indenopyrazoles substituted at R<sup>1</sup> position on antiproliferative activity and the results are summarized in Table 1. Compound **6a**, which has an ethoxy group at R<sup>1</sup> position, exhibited antiproliferative activity with IC<sub>50</sub> values between 20.4 and 60.2 nM. Although compound **6c** containing a hydroxyl group instead of an ethoxy group as the R<sup>1</sup> group did not show a significant antiproliferative activity at 100 nM, compound **2** containing a methoxy group as the R<sup>1</sup> group possessed an antiproliferative activity more potently than compound **6a** (the IC<sub>50</sub> values of compound **2** toward human cancer cell lines: 8.9 ~ 35.6 nM). Furthermore, compound **6p**, which has no substituent on the anilinoquinazoline framework resulted in no significant inhibition at 100 nM, revealing that an alkoxy group at the R<sup>1</sup> position is essential for antiproliferative activity toward the human cancer cells induced by indenopyrazoles.

(Table 1)

We next examined the effect of substituents at the R<sup>2</sup> position of 6-methoxyanilinoquinazolines on the antiproliferative activity. The results are summarized in Table 2. A substituent at 2' (**6e** and **6h**) or 4' (**6j**) position resulted in weak inhibitory effects on antiproliferative activity toward HeLa, PC3, HCT116, and HEK293 cells, whereas 3'-substituted anilinoquinazolines **6g** and **6i** exhibited significant inhibition of antiproliferative activity with IC<sub>50</sub> values between 2.8 and 10.9 nM toward

1  
2  
3  
4  
5  
6  
7  
8  
9  
10  
11  
12  
13  
14  
15  
16  
17  
18  
19  
20  
21  
22  
23  
24  
25  
26  
27  
28  
29  
30  
31  
32  
33  
34  
35  
36  
37  
38  
39  
40  
41  
42  
43  
44  
45  
46  
47  
48  
49  
50  
51  
52  
53  
54  
55  
56  
57  
58  
59  
60

human cancer cells. Interestingly, **6g** did not show significant inhibition toward HEK293 cells at 100 nM. Although 3',4'-dimethoxy-substituted 6-methoxyanilinoquinazoline **6k** showed weak inhibitory effects similar to compound **6j**, 3',5'-dimethoxy-substituted 6-methoxyanilinoquinazoline **6l** exhibited potent inhibition of antiproliferative activity toward HeLa, PC3, HCT116, and HEK293 cells with IC<sub>50</sub> = 3.2, 7.0, 7.4, and 4.6 nM, respectively. The best results were obtained in the case of compound **6m** (GN39482), which has a methoxycarbonyl group at the R<sup>2</sup> position of 6-methoxyanilinoquinazoline and the IC<sub>50</sub> values toward HeLa, PC3, HCT116, and HEK293 cells were 2.47, 2.64, 2.7 and 2.2 nM, respectively. The carboxylic acid derivative **6n** did not show significant inhibition probably due to the difficulty of cell-membrane penetration. A bulky substituent such as an isobutyl group (**6o**) at the R<sup>2</sup> position of 6-methoxyanilinoquinazoline also diminished inhibitory effects on the antiproliferative activity. Needless to say, a 6-methoxy group of anilinoquinazolines is essential for the significant inhibitory potency (**6p** vs. **6q**; **6i** vs. **6r**).

(Table 2)

Because compound **6m** was found to possess a promising antiproliferative activity toward human cancer cells, we next examined antimicrobial activities against *Staphylococcus aureus* 209, *Escherichia coli* HO141, *Candida albicans* JCM1542, *Aspergillus fumigatus* Af293, and *Magnaporthe oryzae* kita-1 and anti-malarial activity against *Plasmodium falciparum* 3D7 by compound **6m**. Recently, antimicrobacterial activities, such as an antitubercular activity, of



indenopyrazoles have been reported.<sup>28,29</sup> Interestingly, compound **6m** did not display any antimicrobial and anti-malarial activities at 100 nM (data not shown). These results indicate that compound **6m** possesses selective inhibition toward human cancer cells. We also investigated the effect of compound **6m** on inhibitory activity for EGFR, KDR, PDGFR $\beta$ , CDK2/CycE1, CDK4/CycD3 and CHK1 kinases to confirm whether **6m** has a potential to inhibit these kinases that have been reported as targets of indenopyrazoles in Figure 1. *In vitro* kinase inhibition assays revealed that compound **6m** showed inhibitory activities toward KDR, PDGFR $\beta$ , and CDK2/CycE1 at 10  $\mu$ M (>82% inhibition). However significant inhibition of compound **6m** toward these kinases was not observed at 0.1  $\mu$ M (See Table S2 in the supporting information).

To clarify the action mechanism of compound **6m** in the antiproliferation of human cancer cell lines, we next analyzed MorphoBase profiling<sup>23,24</sup> and ChemProteoBase profiling<sup>25,26</sup> of compound **6m**. The results of MorphoBase profiling were summarized in Figure 2. Following treatment with compound **6m**, the nuclei were stained with Hoechst33342 and the resulting morphological changes of *src*<sup>ts</sup>-NRK and HeLa cells were segmented and quantified by the IN Cell Analyzer. The phenotypic multiparameters generated were compared with the reference dataset—a compilation of the morphological features induced by 225 compounds—and subjected to statistical analyses, i.e., principal component analysis (PCA), probability scores, and ranking of the top 15 nearest neighbors. Regarding the projection of PCA scores, the phenotypic response of compound **6m** was visible in the

cloud of tubulin inhibitors in the PC1-PC2 scatter plots. Based on the similarity analysis, compound **6m** was also predicted to perturb microtubule dynamics ( $Score_{tubulin} = 1.68$ ) and the typical tubulin inhibitors, such as 9-chloro-5-(2,5-dimethoxyphenyl)-1,3-dihydro-2*H*-benzofuro[3,2-*e*][1,4]diazepin-2-one (NPD8617), (*E*)-1-(6,7-dimethoxy-3,4-dihydroisoquinolin-2(1*H*)-yl)-3-(furan-2-yl)prop-2-en-1-one (NPD6689), vinblastine, and methyl 6-(furan-2-yl)-3-methyl-4-oxo-4,5,6,7-tetrahydrobenzofuran-2-carboxylate (NPD8969),<sup>23</sup> were listed among most of its 15 closest neighbors. These data indicate that the putative molecular target of **6m** is the microtubule system.

(Figure 2)

To verify the predictions, compound **6m** was subjected to ChemProteoBase profiling. The proteomic variation of 296 spots that matched on all gel images was quantified, cosine similarities of compounds in database against compound **6m** was calculated and hierarchical cluster analysis was performed as previously described.<sup>26</sup> As is expected by the MorphoBase profiling, tubulin inhibitors were the most similar compounds to **6m** among 87 compounds in the ChemProteoBase (Figure 3). In hierarchical cluster analysis with 41 standard compounds, compound **6m** was clustered in the cluster with tubulin inhibitors and a TOP2 catalytic inhibitor, which is a different cluster of other type of inhibitors in the database, such as V-ATPase inhibitors and proteasome inhibitors (Figure 3).

(Figure 3)

Since tubulins have been suggested as one of the target proteins of compound **6m** by both MorphoBase profiling and ChemProteoBase profiling analyses, we next examined effect of compound **6m** on tubulin polymerization *in vitro*. Vinblastine (10  $\mu$ M) and paclitaxel (2  $\mu$ M) were used as positive controls, respectively. As shown in Figure 4, compound **6m** inhibited tubulin polymerization in a concentration-dependent manner in a range of 3-30  $\mu$ M. It is known that tubulin inhibitors induced G2/M cell cycle arrest.<sup>30</sup> Therefore, we examined the effect of compound **6m** on the cell cycle in HeLa cells. HeLa cells were treated with compounds at various concentrations for 24 h and stained with propidium iodide (PI) and RNase A for 30 min. The analysis of the DNA content of the cells was performed by flow cytometry. As shown in Figure 5, compound **6m** arrested cell cycles at G2/M stage similar to colchicine known as a tubulin polymerization inhibitor. It should be noted that cell cycles were not affected by compound **6p** which was used as a negative control.

(Figure 4)

(Figure 5)

We next examined the western blotting analysis of acetylated tubulins and the immunofluorescence of microtubules to confirm whether compound **6m** inhibits tubulin polymerization in cells. It is known that acetylation of Lys 40 in  $\alpha$ -tubulin is necessary process for microtubule formation. Therefore, effects of compound **6m** on acetylated tubulin accumulation and microtubule dynamics were examined by western blot analysis and immunofluorescence with the specific tubulin antibody

1  
2  
3  
4  
5  
6 using HeLa cells, respectively. The results are shown in Figure 6. Colchicine, a positive control,  
7  
8  
9 arrested acetylated tubulin accumulation in a range of 30-100 nM. Interestingly, compound **6m**  
10  
11 inhibited the acetylated tubulin accumulation in a similar manner to colchicine (Figure 6a). We also  
12  
13 examined the effects of compounds **6o**, **2**, and **6q** on acetylated tubulin accumulation. Compound **6o**,  
14  
15 which exhibited a 10-fold weaker proliferative activity than compound **6m**, inhibited the acetylated  
16  
17 tubulin accumulation at 300 nM. However, compounds **2** and **6q** did not display significant  
18  
19 inhibition of the acetylated tubulin accumulation even at 1000 nM.  
20  
21  
22  
23  
24  
25

26 Figure 6b shows immunofluorescence analysis of microtubule formation using the tubulin-specific  
27  
28 antibody. Colchicine inhibited microtubule formation, whereas paclitaxel did not affect the  
29  
30 microtubule formation at 100 nM. It is known that paclitaxel stabilizes microtubule formation and  
31  
32 arrests tubulin depolymerization process. Compound **6m** exhibited microtubule formation similar to  
33  
34 colchicine at 30 nM. Compound **6o**, which inhibited acetylated tubulin accumulation at 300 nM, also  
35  
36 exhibited microtubule formation at the same concentration (300 nM). However, compound **2**, which  
37  
38 did not affect acetylated tubulin accumulation at 1,000 nM, showed no effect on microtubule  
39  
40 formation at the same concentration (1,000 nM). These results suggest that compound **6m** inhibits  
41  
42 antiproliferative activity toward human cancer cells probably by inhibiting tubulin polymerization  
43  
44 process in the cells. Compound **6o** also inhibited acetylated tubulin accumulation and microtubule  
45  
46 formation at ten-fold higher concentration (300 nM) than compound **6m** and this is reflected in the  
47  
48  
49  
50  
51  
52  
53  
54  
55  
56  
57  
58  
59  
60

antiproliferative effect by compounds **6m** and **6o**. Indeed, their IC<sub>50</sub> values toward HeLa cells are 2.47 and 19.95 nM, respectively.

(Figure 6)

## Conclusion

We developed compound **6m** as a potent cell growth inhibitor by SAR based on the structure of indenopyrazole **2**. Both a methoxy group at R<sup>1</sup> position and a methoxycarbonyl group at R<sup>2</sup> position of the anilinoquinazoline framework are essential for the high cell growth inhibition. Compound **6m** was found to possess a promising antiproliferative activity toward human cancer cells without affecting any anti-microbial and anti-malarial activities at 100 nM. We clarified the action mechanism of cell growth inhibition induced by compound **6m** using MorphoBase and ChemProteoBase profiling methods. MorphoBase profiling analysis revealed that the phenotypic response of compound **6m** was visible in the cloud of tubulin inhibitors in the PC1-PC2 scatter plots, predicting to perturb microtubule dynamics ( $Score_{tubulin} = 1.68$ ). ChemProteoBase profiling analysis also suggested that tubulin inhibitors were the most similar compounds to **6m** among 87 compounds in the database. Indeed, compound **6m** inhibited tubulin polymerization in a concentration-dependent manner and induced G2/M cell cycle arrest in HeLa cells. Furthermore, compound **6m** inhibited the acetylated tubulin accumulation and the microtubule formation in a similar manner to colchicine in HeLa cells, revealing that a promising antiproliferative activity of

compound **6m** toward human cancer cells is probably caused by the tubulin polymerization inhibition. Although indenopyrazoles have been reported as central nervous system agents, kinase inhibitors, and antibacterial agents, this is the first to observe tubulin polymerization inhibition by indenopyrazoles. The current findings suggest that the indenopyrazole framework is a possible candidate for development of biologically active molecules in the pharmaceutical drug design.

## Experimental section

### General Information

Analytical thin layer chromatography (TLC) was performed on a glass plates of silica gel 60 GF<sub>254</sub> (Merck), which were visualized by the quenching of UV fluorescence (254 nm), and/or by an aqueous alkaline KMnO<sub>4</sub> solution followed by heating. Column chromatography was conducted on silica gel (Merck Kieselgel 70-230 mesh). Most commercially supplied chemicals were used without further purification. <sup>1</sup>H and <sup>13</sup>C NMR spectra were recorded on a Bruker biospin AVANCE II (400 MHz) or a VARIAN UNITY-INOVA 400 (400 MHz) spectrometer. The chemical shifts are reported in δ units relative to internal tetramethylsilane. IR spectra were recorded on a JASCO FT/IR-4100 spectrometer. Liquid chromatogram mass spectrometer was recorded on Shimadzu LCMS-2010EV. High-resolution mass spectra (ESI) were recorded on a Bruker Daltonics micro TOF-15 focus. Purity of all final compounds was determined by HPLC analysis with a Hiber LiChrosorb Si60 5 μm

(Cica-MERCK) with UV detection at 254 nm or elemental analysis performed by a CE instrument

EA1110 CHNS-O automatic elemental analyser, with the purity all being higher than 95%.

***tert*-Butyl(2-isothiocyanatophenoxy)dimethylsilane (4a)**

A mixture of 2-((*tert*-butyldimethylsilyl)oxy)aniline (0.208 g, 0.93 mmol) and phenyl chlorothionoformate (0.065 mL, 0.47 mmol) in THF (5 mL) was stirred 2h at room temperature. The reaction was quenched with water and the mixture was extracted with EtOAc. The organic layer was washed with water and brine, dried over anhydrous Na<sub>2</sub>SO<sub>4</sub>, and concentrated. To the residue dissolved in toluene (5 mL) were added TEA (0.13 mL, 0.9 mmol) and Cl<sub>3</sub>SiH (0.09 mL, 0.9 mmol) under N<sub>2</sub> and the mixture was stirred for 2 h at room temperature. The reaction was quenched with water and the precipitate was filtered off. The mixture was extracted with EtOAc and the organic layer was washed with water and brine, dried over anhydrous Na<sub>2</sub>SO<sub>4</sub>, and concentrated. The residue was purified by column chromatography with hexane to give *tert*-butyl(2-isothiocyanatophenoxy)dimethylsilane (**4a**) as a colorless oil, quantitatively. <sup>1</sup>H NMR (400 MHz, CDCl<sub>3</sub>): δ 7.16-7.11 (2H, m), 6.92-6.87 (2H, m), 1.03 (9H, s), 0.29 (6H, s); <sup>13</sup>CNMR (100 MHz, CDCl<sub>3</sub>): δ 152.1, 136.6, 128.1, 126.3, 123.0, 121.5, 120.0, 25.7, 18.4, -4.2; IR (NaCl) 3734, 2930, 2858, 2360, 2076, 1507, 1490, 1472, 1456, 1289, 1255, 1225, 1109 cm<sup>-1</sup>; HRMS (ESI, positive) *m/z* calcd. for C<sub>13</sub>H<sub>19</sub>NOSSi [M+Na]<sup>+</sup>: 288.0849, found: 288.0848.

***tert*-Butyl(3-isothiocyanatophenoxy)dimethylsilane (4b)**

This compound was prepared from 3-((*tert*-butyldimethylsilyl)oxy)aniline (0.929 g, 4.2 mmol), chlorothionoformate (0.29 mL, 2.1 mmol), TEA (0.47 mL, 3.4 mmol), and Cl<sub>3</sub>SiH (0.34 mL, 3.4 mmol) using the procedure described for **4a**. Purification by column chromatography (Hexane:EtOAc = 100:1 v/v) gave *tert*-butyl(3-isothiocyanatophenoxy)dimethylsilane (**4b**) as a colorless oil, quantitatively. <sup>1</sup>H NMR (400 MHz, CDCl<sub>3</sub>): δ 7.18 (1H, dd, *J* = 8.0, 8.4 Hz), 6.84 (1H, d, *J* = 8.0 Hz), 6.76 (1H, d, *J* = 8.0 Hz), 6.69 (1H, s), 0.98 (9H, s), 0.21 (6H, s); <sup>13</sup>CNMR (100 MHz, CDCl<sub>3</sub>): δ 156.5, 135.1, 131.9, 130.1, 119.5, 118.9, 117.4, 25.6, 18.1, -4.2; IR (NaCl) 3734, 2955, 2930, 2858, 2360, 2112, 1592, 1486, 1472, 1294, 1254, 1184, 1153, 1006 cm<sup>-1</sup>; HRMS (ESI, positive) *m/z* calcd. for C<sub>13</sub>H<sub>19</sub>NOSSi [M+H]<sup>+</sup>: 266.1029, found: 266.1036.

**1-Isothiocyanato-3,5-dimethoxybenzene (4c)**

This compound was prepared from 3,5-dimethoxyaniline (0.153 g, 1 mmol), phenyl chlorothionoformate (0.07 mL, 0.5 mmol), TEA (0.11 mL, 0.77 mmol), and Cl<sub>3</sub>SiH (0.08 mL, 0.77 mmol) using the procedure described for **4a**. Purification by column chromatography (hexane:EtOAc = 80:1 v/v) gave 1-isothiocyanato-3,5-dimethoxybenzene (**4c**) as a white solid (0.0896 g, 0.49 mmol, 96%). mp: 48-49 °C; <sup>1</sup>H NMR (400 MHz, CDCl<sub>3</sub>): δ 6.37 (3H, s), 3.77 (3H,



s);  $^{13}\text{C}$ NMR (100 MHz,  $\text{CDCl}_3$ ):  $\delta$  161.1, 135.4, 132.5, 104.0, 100.3, 55.5; IR (NaCl) 3099, 3006, 2967, 2941, 2840, 2360, 2147, 1598, 1458, 1422, 1353, 1304, 1208, 1192, 1156, 1062, 1006  $\text{cm}^{-1}$ ; HRMS (ESI, positive)  $m/z$  calcd. for  $\text{C}_9\text{H}_9\text{NO}_2\text{S}$   $[\text{M}+\text{H}]^+$ : 196.0427, found: 196.0432.

#### Methyl 3-isothiocyanatobenzoate (**4d**)

This compound was prepared from methyl 3-aminobenzoate (0.151 g, 1 mmol), chlorothionoformate (0.07 mL, 0.5 mmol), TEA (0.17 mL, 1.2 mmol), and  $\text{Cl}_3\text{SiH}$  (0.12 mL, 1.2 mmol) using the procedure described for **4a**. Purification by column chromatography (hexane:EtOAc = 50:1 v/v) gave methyl 3-isothiocyanatobenzoate (**4d**) as a colorless oil, quantitatively.  $^1\text{H}$  NMR (400 MHz,  $\text{CDCl}_3$ ):  $\delta$  7.91 (1H, d,  $J$  = 7.2 Hz), 7.89 (1H, s), 7.46-7.38 (2H, m), 3.94 (3H, s);  $^{13}\text{C}$ NMR (100 MHz,  $\text{CDCl}_3$ ):  $\delta$  165.3, 137.1, 131.7, 129.6, 128.1, 126.6, 52.4; IR (NaCl) 3734, 2955, 2360, 2090, 1727, 1582, 1443, 1292, 1224, 1104, 1077, 1000  $\text{cm}^{-1}$ ; HRMS (ESI, positive)  $m/z$  calcd. for  $\text{C}_9\text{H}_7\text{NO}_2\text{S}$   $[\text{M}+\text{H}]^+$ : 194.0270, found: 194.0266.

#### 1-Isobutoxy-3-isothiocyanatobenzene (**4e**)

This compound was prepared from 3-isobutoxyaniline (0.151 g, 1 mmol), chlorothionoformate (0.05 mL, 0.38 mmol), TEA (0.15 mL, 1.1 mmol), and  $\text{Cl}_3\text{SiH}$  (0.11 mL, 1.1 mmol) using the procedure described for **4a**. Purification by column chromatography (hexane:EtOAc = 100:1 v/v) gave

1-isobutoxy-3-isothiocyanatobenzene (**4e**) as a light yellow oil, quantitatively.  $^1\text{H}$  NMR (400 MHz,  $\text{CDCl}_3$ ):  $\delta$  7.22 (1H, dd,  $J = 8.0, 8.0$  Hz), 6.83-6.79 (2H, m), 6.74 (1H, s), 3.70 (2H, d,  $J = 6.4$  Hz), 2.13-2.03 (1H, m), 1.02 (6H, d,  $J = 6.4$  Hz);  $^{13}\text{C}$  NMR (100 MHz,  $\text{CDCl}_3$ ):  $\delta$  160.0, 135.3, 132.0, 130.1, 117.8, 114.2, 111.7, 74.6, 28.2, 19.2; IR (NaCl) 2959, 2872, 2100, 1600, 1488, 1470, 1394, 1313, 1287, 1267, 1185, 1155, 1038  $\text{cm}^{-1}$ ; HRMS (ESI, positive)  $m/z$  calcd. for  $\text{C}_{11}\text{H}_{13}\text{NOS}$   $[\text{M}+\text{H}]^+$ : 208.0791, found: 208.0796.

#### 6-Ethoxy-*N*-phenyl-1,4-dihydroindeno[1,2-*c*]pyrazol-3-amine (**6a**)

To a mixture of 5-ethoxy-2,3-dihydro-1H-inden-1-one (0.103 g, 0.58 mmol) and phenyl isothiocyanate (0.07 mL, 0.58 mmol) in THF was added LiHMDS, which was prepared from 1.6 M hexane solution of *n*-BuLi (0.36 mL, 0.58 mmol) and HMDS (0.12 mL, 0.58 mmol) with stirring at 0 °C for 30 min, dropwise at room temperature and the mixture was stirred for 12 h. Hydrazine (0.03 mL, 0.58 mmol) and acetic acid (0.03 mL) were added and the reaction mixture was refluxed for 24 h. The reaction was quenched with water and the mixture was extracted with EtOAc. The organic layer was washed with aqueous  $\text{NaHCO}_3$ , water, and brine, dried over anhydrous  $\text{Na}_2\text{SO}_4$ , and concentrated. The residue was purified by column chromatography with  $\text{CH}_2\text{Cl}_2$  to give 6-ethoxy-*N*-phenyl-1,4-dihydroindeno[1,2-*c*]pyrazol-3-amine (**6a**) as a yellow solid (0.0825 g, 0.28 mmol, 48%). mp: 74-75 °C;  $^1\text{H}$  NMR (400 MHz,  $\text{CDCl}_3$ ):  $\delta$  7.38 (1H, d,  $J = 8.0$  Hz), 7.21 (2H,

dd,  $J = 7.6, 8.4$  Hz), 6.94 (1H, s), 6.90-6.85 (3H, m), 6.72 (1H, d,  $J = 8.4$  Hz), 4.00 (2H, q,  $J = 7.2$  Hz), 3.33 (2H, s), 1.41 (3H, t,  $J = 7.2$  Hz);  $^{13}\text{C}$ NMR (100 MHz,  $\text{CDCl}_3$ ):  $\delta$  158.2, 155.3, 150.7, 143.1, 141.8, 129.2, 126.2, 120.1, 120.0, 116.1, 112.8, 112.4, 110.9, 63.6, 30.4, 14.9; IR (NaCl) 3734, 3053, 2979, 2900, 2360, 1600, 1540, 1508, 1497, 1464, 1394, 1309, 1241, 1111, 1043  $\text{cm}^{-1}$ ; HRMS (ESI, positive)  $m/z$  calcd. for  $\text{C}_{18}\text{H}_{17}\text{N}_3\text{O}$   $[\text{M}+\text{H}]^+$ : 292.1444, found: 292.1445; HPLC purity: 99.7%, retention time: 6.96 min, The eluents were mixture of MeOH and  $\text{CH}_2\text{Cl}_2$  (1:4).

#### 6-((*tert*-Butyldimethylsilyl)oxy)-*N*-phenyl-1,4-dihydroindeno[1,2-*c*]pyrazol-3-amine (6b)

This compound was prepared from 5-((*tert*-butyldimethylsilyl)oxy)-2,3-dihydro-1H-inden-1-one (**3**) (0.249 g, 0.95 mmol) and phenyl isothiocyanate (0.11 mL, 0.95 mmol) using the procedure described for **6a**. Purification by column chromatography (hexane:EtOAc = 2:1 v/v) gave 6-((*tert*-butyldimethylsilyl)oxy)-*N*-phenyl-1,4-dihydroindeno[1,2-*c*]pyrazol-3-amine (**6b**) as a light brown solid (0.197 g, 0.52 mmol, 55%). mp: 93-94  $^{\circ}\text{C}$ ;  $^1\text{H}$  NMR (400 MHz,  $\text{CDCl}_3$ ):  $\delta$  7.42 (1H, d,  $J = 8.4$  Hz), 7.28-7.25 (3H, m), 6.99 (2H, d,  $J = 8.0$  Hz), 6.94 (1H, s), 6.91 (1H, dd,  $J = 7.6, 7.2$  Hz), 6.78 (1H, d,  $J = 8.0$  Hz), 6.01 (1H, bs), 3.41 (2H, s), 0.99 (9H, s), 0.21 (6H, s);  $^{13}\text{C}$ NMR (100 MHz,  $\text{CDCl}_3$ ):  $\delta$  155.3, 154.9, 150.7, 143.1, 141.9, 129.2, 126.8, 120.08, 120.05, 118.5, 117.9, 116.1, 111.4, 30.2, 25.7, 18.2, -4.4; IR (NaCl) 3181, 3051, 2955, 2929, 2896, 2858, 2360, 1600, 1530, 1497, 1463, 1444, 1418, 1396, 1281, 1250, 1086  $\text{cm}^{-1}$ ; HRMS (ESI, positive)  $m/z$  calcd. for  $\text{C}_{22}\text{H}_{27}\text{N}_3\text{OSi}$

[M+H]<sup>+</sup>: 378.1996, found: 378.1994.

**3-(Phenylamino)-1,4-dihydroindeno[1,2-c]pyrazol-6-ol (6c)**

To a solution of **6b** (0.17 g, 0.45 mmol) in MeOH (10 mL) was added TBAF (1M solution of THF, 0.81 mL, 0.81 mmol) and the mixture was stirred 2 h at room temperature. The reaction mixture was extracted with EtOAc and the organic layer was washed with aqueous NH<sub>4</sub>Cl, water, and brine, dried over anhydrous Na<sub>2</sub>SO<sub>4</sub>, and concentrated. The residue was purified by column chromatography (CH<sub>2</sub>Cl<sub>2</sub>:MeOH = 50:1 v/v) to give 3-(phenylamino)-1,4-dihydroindeno[1,2-c]pyrazol-6-ol (**6c**) as a light yellow solid (0.114 g, 0.43 mmol, 96%). mp: 150-151 °C; <sup>1</sup>H NMR (400 MHz, CD<sub>3</sub>OD): δ 7.41 (1H, d, *J* = 8.4 Hz), 7.21 (2H, dd, *J* = 7.6, 7.6 Hz), 7.00 (2H, d, *J* = 7.6 Hz), 6.91 (1H, s), 6.80 (1H, dd, *J* = 7.2, 7.6 Hz), 6.75 (1H, d, *J* = 8.4 Hz), 3.38 (2H, s), 3.34 (1H, s); <sup>13</sup>CNMR (100 MHz, CD<sub>3</sub>OD): δ 156.6, 155.6, 151.0, 143.7, 141.6, 128.7, 125.3, 119.6, 119.3, 115.4, 113.4, 113.0, 110.3, 29.3; IR (KBr) 3376, 3052, 2896, 2810, 2362, 1620, 1600, 1528, 1497, 1449, 1243, 1104, 1082 cm<sup>-1</sup>; HRMS (ESI, positive) *m/z* calcd. for C<sub>16</sub>H<sub>13</sub>N<sub>3</sub>O [M+H]<sup>+</sup>: 264.1131, found: 264.1132; HPLC purity: 98.3%, retention time: 7.69 min (MeOH:CH<sub>2</sub>Cl<sub>2</sub> = 1:4).

***N*-(2-((tert-butyldimethylsilyl)oxy)phenyl)-6-methoxy-1,4-dihydroindeno[1,2-c]pyrazol-3-amine (**6d**)**

This compound was prepared from 5-methoxy-1-indanone (0.078 g, 0.48 mmol) and *tert*-butyl(2-isothiocyanatophenoxy)dimethylsilane (**4a**) (0.127 g, 0.48 mmol) using the procedure described for **6a**. Purification by column chromatography with (hexane:EtOAc = 5:1 v/v) gave *N*-(2-((*tert*-butyldimethylsilyl)oxy)phenyl)-6-methoxy-1,4-dihydroindeno[1,2-*c*]pyrazol-3-amine (**6d**) as a yellow solid (0.0565 g, 0.14 mmol, 29%). mp: 72-73 °C; <sup>1</sup>H NMR (400 MHz, CDCl<sub>3</sub>): δ 7.51 (1H, d, *J* = 8.0 Hz), 7.36 (1H, d, *J* = 6.8 Hz), 7.04 (1H, s), 6.95-6.83 (3H, m), 6.76 (1H, dd, *J* = 8.0, 7.2 Hz), 6.26 (1H, bs), 3.85 (3H, s), 3.48 (2H, s), 1.06 (9H, s), 0.28 (6H, s); <sup>13</sup>CNMR (100 MHz, CDCl<sub>3</sub>): δ 158.9, 153.9, 150.7, 143.2, 142.7, 134.9, 126.2, 121.9, 120.0, 119.5, 118.1, 115.2, 112.2, 112.1, 111.9, 55.5, 29.8, 25.9, 18.3, -4.3; IR (NaCl) 3423, 3063, 2929, 2857, 2360, 1598, 1537, 1495, 1460, 1283, 1250, 1106, 1082, 1035 cm<sup>-1</sup>; HRMS (ESI, positive) *m/z* calcd. for C<sub>23</sub>H<sub>29</sub>N<sub>3</sub>O<sub>2</sub>Si [M+H]<sup>+</sup>: 408.2102, found: 408.2105;

#### 2-((6-Methoxy-1,4-dihydroindeno[1,2-*c*]pyrazol-3-yl)amino)phenol (**6e**)

This compound was prepared from *N*-(2-((*tert*-butyldimethylsilyl)oxy)phenyl)-6-methoxy-1,4-dihydroindeno[1,2-*c*]pyrazol-3-amine (**6d**) (0.057 g, 0.14 mmol) and TBAF (1M in THF; 0.25 mL, 0.25 mmol) using the procedure described for **6c**. Purification by column chromatography with (CH<sub>2</sub>Cl<sub>2</sub>:MeOH = 50:1 v/v) gave 2-((6-methoxy-1,4-dihydroindeno[1,2-*c*]pyrazol-3-yl)amino)phenol (**6e**) as a dark green solid

(0.0195 g, 0.066 mmol, 47%). mp: 196-197 °C; <sup>1</sup>H NMR (400 MHz, CD<sub>3</sub>OD): δ 7.50 (1H, d, *J* = 8.0 Hz), 7.10 (1H, d, *J* = 7.6 Hz), 7.05 (1H, s), 6.88 (1H, d, *J* = 8.4 Hz), 6.84-6.72 (3H, m), 3.81 (3H, s), 3.44 (2H, s); <sup>13</sup>CNMR (100 MHz, CD<sub>3</sub>OD): δ 159.3, 155.5, 150.8, 145.6, 142.0, 131.7, 126.3, 120.1, 119.6, 119.4, 115.6, 114.4, 112.1, 111.6, 109.8, 54.5, 29.5; IR (KBr) 3368, 3241, 2830, 2682, 2499, 1589, 1510, 1471, 1400, 1310, 1286, 1246, 1112, 1090, 1038 cm<sup>-1</sup>; HRMS (ESI, positive) *m/z* calcd. for C<sub>17</sub>H<sub>15</sub>N<sub>3</sub>O<sub>2</sub> [M+H]<sup>+</sup>: 294.1237, found: 294.1241; HPLC purity: 98.8%, retention time: 10.65 min (MeOH:CH<sub>2</sub>Cl<sub>2</sub> = 1:1).

***N*-(3-((*tert*-butyldimethylsilyl)oxy)phenyl)-6-methoxy-1,4-dihydroindeno[1,2-*c*]pyrazol-3-amine (6f)**

This compound was prepared from 5-methoxy-1-indanone (0.224 g, 1.38 mmol) and *tert*-butyl(3-isothiocyanatophenoxy)dimethylsilane (**4b**) (0.366 g, 1.38 mmol) using the procedure described for **6a**. Purification by column chromatography with (hexane:EtOAc = 2:1 v/v) gave *N*-(3-((*tert*-butyldimethylsilyl)oxy)phenyl)-6-methoxy-1,4-dihydroindeno[1,2-*c*]pyrazol-3-amine (**6f**) as a yellow solid (0.386 g, 0.946 mmol, 68%). mp: 136-137 °C; <sup>1</sup>H NMR (400 MHz, CDCl<sub>3</sub>): δ 7.50 (1H, d, *J* = 8.0 Hz), 7.10 (1H, dd, *J* = 8.0, 8.0 Hz), 7.03 (1H, s), 6.87 (1H, d, *J* = 6.8 Hz), 6.61 (1H, d, *J* = 6.8 Hz), 6.52 (1H, s), 6.40 (1H, d, *J* = 8.0 Hz), 5.94 (1H, bs), 3.85 (3H, s), 3.47 (2H, s), 0.97 (9H, s), 0.19 (6H, s); <sup>13</sup>CNMR (100 MHz, CDCl<sub>3</sub>): δ 158.9, 156.7, 155.1, 150.7, 144.4, 141.8,

129.8, 126.3, 120.1, 112.1, 111.9, 111.8, 109.4, 108.0, 55.4, 30.4, 25.7, 18.1, -4.4; IR (NaCl) 3063, 2954, 2929, 2858, 2360, 1600, 1524, 1490, 1471, 1310, 1283, 1250, 1181, 1155, 1083, 1035  $\text{cm}^{-1}$ ; HRMS (ESI, positive)  $m/z$  calcd. for  $\text{C}_{23}\text{H}_{29}\text{N}_3\text{O}_2\text{Si}$   $[\text{M}+\text{H}]^+$ : 408.2102, found: 408.2104;

**3-((6-Methoxy-1,4-dihydroindeno[1,2-c]pyrazol-3-yl)amino)phenol (6g)**

This compound was prepared from

*N*-(3-((tert-butyldimethylsilyl)oxy)phenyl)-6-methoxy-1,4-dihydroindeno[1,2-c]pyrazol-3-amine

(**6f**) (0.386 g, 0.94 mmol) and TBAF (1M in THF; 1.69 mL, 1.69 mmol) using the procedure

described for **6c**. Purification by column chromatography with ( $\text{CH}_2\text{Cl}_2$ :MeOH = 50:1 v/v) gave

3-((6-methoxy-1,4-dihydroindeno[1,2-c]pyrazol-3-yl)amino)phenol (**6g**) as a white solid,

quantitatively. mp: 201-202  $^{\circ}\text{C}$ ;  $^1\text{H}$  NMR (400 MHz,  $\text{CD}_3\text{OD}$ ):  $\delta$  7.52 (1H, d,  $J$  = 8.0 Hz), 7.09 (1H,

s), 7.05 (1H, dd,  $J$  = 8.0, 8.0 Hz), 6.90 (1H, d,  $J$  = 8.4 Hz), 6.52-6.49 (2H, m), 6.31 (1H, d,  $J$  = 8.0

Hz), 3.83 (3H, s), 3.47 (2H, s);  $^{13}\text{C}$  NMR (100 MHz,  $\text{CD}_3\text{OD}$ ):  $\delta$  159.3, 157.9, 155.5, 150.9, 145.1,

141.2, 129.5, 126.4, 119.4, 112.1, 111.6, 110.7, 107.2, 106.4, 102.3, 54.6, 29.5; IR (KBr) 3402, 3347,

3058, 2944, 2900, 2826, 2703, 1615, 1600, 1543, 1463, 1267, 1250, 1157, 1108, 1075, 1039  $\text{cm}^{-1}$ ;

HRMS (ESI, positive)  $m/z$  calcd. for  $\text{C}_{17}\text{H}_{15}\text{N}_3\text{O}_2$   $[\text{M}+\text{H}]^+$ : 294.1237, found: 294.1245; HPLC

purity: 99.9%, retention time: 10.65 min (MeOH: $\text{CH}_2\text{Cl}_2$  = 1:1).

**6-Methoxy-*N*-(2-methoxyphenyl)-1,4-dihydroindeno[1,2-c]pyrazol-3-amine (6h)**

This compound was prepared from 5-methoxy-1-indanone (0.08 g, 0.5 mmol) and 1-isothiocyanato-2-methoxybenzene (0.082 g, 0.5 mmol) using the procedure described for **6a**. Purification by column chromatography with (hexane:EtOAc = 2:1 v/v) gave 6-methoxy-*N*-(2-methoxyphenyl)-1,4-dihydroindeno[1,2-*c*]pyrazol-3-amine (**6h**) as a light yellow solid (0.0615 g, 0.2 mmol, 40%). mp: 182-183 °C; <sup>1</sup>H NMR (400 MHz, CDCl<sub>3</sub>): δ 7.55 (1H, d, *J* = 8.4 Hz), 7.06 (1H, s), 6.97-6.86 (5H, m), 6.39 (1H, bs), 3.94 (3H, s), 3.87 (3H, s), 3.53 (2H, s); <sup>13</sup>CNMR (100 MHz, CDCl<sub>3</sub>): δ 159.0, 155.0, 150.7, 147.3, 141.6, 133.0, 126.5, 121.1, 120.0, 119.5, 114.3, 112.4, 112.0, 112.0, 110.2, 55.6, 55.5, 30.1; IR (NaCl) 3064, 2933, 2834, 2360, 1600, 1532, 1461, 1310, 1283, 1245, 1112, 1030 cm<sup>-1</sup>; HRMS (ESI, positive) *m/z* calcd. for C<sub>18</sub>H<sub>17</sub>N<sub>3</sub>O<sub>2</sub> [M+H]<sup>+</sup>: 308.1394, found: 308.1399; HPLC purity: 99.9%, retention time: 6.91 min, The eluents were mixture of MeOH and CH<sub>2</sub>Cl<sub>2</sub> (1:9).

#### 6-Methoxy-*N*-(3-methoxyphenyl)-1,4-dihydroindeno[1,2-*c*]pyrazol-3-amine (**6i**)

This compound was prepared from 5-methoxy-1-indanone (0.1 g, 0.62 mmol) and 3-methoxyphenyl isothiocyanate (0.087 mL, 0.62 mmol) using the procedure described for **6a**. Purification by column chromatography with (CH<sub>2</sub>Cl<sub>2</sub>:MeOH = 30:1 v/v) gave 6-methoxy-*N*-(3-methoxyphenyl)-1,4-dihydroindeno[1,2-*c*]pyrazol-3-amine (**6i**) as a white solid (0.113 g, 0.37 mmol, 60%). mp: 153-154 °C; <sup>1</sup>H NMR (400 MHz, CDCl<sub>3</sub>): δ 7.50 (1H, d, *J* = 8.4 Hz), 7.19 (1H, dd,



$J = 8.4, 8.4$  Hz), 7.04 (1H, s), 6.88 (1H, d,  $J = 8.4$  Hz), 6.60-6.59 (2H, m), 6.49 (1H, d,  $J = 7.6$  Hz), 6.07 (1H, bs), 3.86 (3H, s), 3.79 (3H, s), 3.49 (2H, s);  $^{13}\text{C}$ NMR (100 MHz,  $\text{CDCl}_3$ ):  $\delta$  160.7, 158.9, 155.0, 150.7, 144.5, 141.7, 130.0, 126.2, 120.0, 112.3, 111.9, 111.7, 108.6, 105.6, 101.7, 55.5, 55.2, 30.3; IR (NaCl) 3004, 2904, 2834, 2360, 1601, 1524, 1494, 1310, 1284, 1248, 1202, 1158, 1082, 1034  $\text{cm}^{-1}$ ; HRMS (ESI, positive)  $m/z$  calcd. for  $\text{C}_{18}\text{H}_{17}\text{N}_3\text{O}_2$   $[\text{M}+\text{H}]^+$ : 308.1394, found: 308.1389; HPLC purity: 97.7%, retention time: 7.74 min (MeOH:  $\text{CH}_2\text{Cl}_2 = 1:9$ ).

#### 6-Methoxy-*N*-(4-methoxyphenyl)-1,4-dihydroindeno[1,2-*c*]pyrazol-3-amine (6j)

This compound was prepared from 5-methoxy-1-indanone (0.2 g, 0.123 mmol) and 4-methoxyphenyl isothiocyanate (0.17 mL, 1.23 mmol) using the procedure described for **6a**. Purification by column chromatography with (hexane:EtOAc = 1:1 v/v) gave 6-methoxy-*N*-(4-methoxyphenyl)-1,4-dihydroindeno[1,2-*c*]pyrazol-3-amine (**6j**) as a white solid (0.141 g, 0.46 mmol, 37%). mp: 137-138 °C;  $^1\text{H}$  NMR (400 MHz,  $\text{CDCl}_3$ ):  $\delta$  7.50 (1H, d,  $J = 8.4$  Hz), 7.05-7.03 (3H, m), 6.89-6.87 (3H, m), 5.81 (1H, bs), 3.86 (3H, s), 3.82 (3H, s), 3.40 (2H, s);  $^{13}\text{C}$ NMR (100 MHz,  $\text{CDCl}_3$ ):  $\delta$  158.8, 155.5, 154.2, 150.8, 143.3, 136.5, 126.5, 120.1, 118.8, 114.5, 112.1, 111.8, 109.6, 55.6, 55.4, 30.3; IR (NaCl) 3182, 2903, 2832, 2360, 1615, 1509, 1466, 1310, 1282, 1240, 1179, 1082, 1034  $\text{cm}^{-1}$ ; HRMS (ESI, positive)  $m/z$  calcd. for  $\text{C}_{18}\text{H}_{17}\text{N}_3\text{O}_2$   $[\text{M}+\text{H}]^+$ : 308.1394, found: 308.1393; HPLC purity: 97.9%, retention time: 11.04 min (MeOH: $\text{CH}_2\text{Cl}_2 = 3:97$ ).

***N*-(3,4-dimethoxyphenyl)-6-methoxy-1,4-dihydroindeno[1,2-*c*]pyrazol-3-amine (6k)**

This compound was prepared from 5-methoxy-1-indanone (0.2 g, 0.123 mmol) and 3,4-dimethoxyphenyl isothiocyanate (0.24 g, 1.23 mmol) using the procedure described for **6a**.

Purification by column chromatography with (CH<sub>2</sub>Cl<sub>2</sub>:MeOH = 100:1 v/v) gave

*N*-(3,4-dimethoxyphenyl)-6-methoxy-1,4-dihydroindeno[1,2-*c*]pyrazol-3-amine (**6k**) as a light

brown solid (0.202 g, 0.6 mmol, 49%). mp: 102-103 °C; <sup>1</sup>H NMR (400 MHz, CDCl<sub>3</sub>): δ 7.51 (1H, d,

*J* = 8.4 Hz), 7.04 (1H, s), 6.89 (1H, d, *J* = 8.4 Hz), 6.83 (1H, d, *J* = 8.4 Hz), 6.71 (1H, s), 6.61 (1H, d,

*J* = 8.4 Hz), 5.85 (1H, bs), 3.88 (3H, s), 3.86 (6H, s), 3.42 (2H, s); <sup>13</sup>CNMR (100 MHz, CDCl<sub>3</sub>): δ

158.9, 155.5, 150.7, 149.7, 143.6, 143.0, 137.0, 126.3, 120.0, 112.4, 112.2, 111.9, 109.9, 108.7,

102.6, 56.4, 55.7, 55.4, 30.3; IR (NaCl) 3337, 3014, 2934, 2833, 1612, 1511, 1466, 1310, 1282,

1232, 1165, 1134, 1082, 1027 cm<sup>-1</sup>; HRMS (ESI, positive) *m/z* calcd. for C<sub>19</sub>H<sub>19</sub>N<sub>3</sub>O<sub>3</sub> [M+H]<sup>+</sup>:

338.1499, found: 338.1503; HPLC purity: 96.0%, retention time: 8.28 min (MeOH:CH<sub>2</sub>Cl<sub>2</sub> = 1:9).

***N*-(3,5-dimethoxyphenyl)-6-methoxy-1,4-dihydroindeno[1,2-*c*]pyrazol-3-amine (6l)**

This compound was prepared from 5-methoxy-1-indanone (0.08 g, 0.49 mmol) and

1-isothiocyanato-3,5-dimethoxybenzene (**2c**) (0.0896 g, 0.49 mmol) using the procedure described

for **6a**. Purification by column chromatography with hexane:EtOAc = 1:1 v/v) gave

*N*-(3,4-dimethoxyphenyl)-6-methoxy-1,4-dihydroindeno[1,2-*c*]pyrazol-3-amine (**6l**) as a light brown solid (0.0827 g, 0.245 mmol, 50%). mp: 88-89 °C; <sup>1</sup>H NMR (400 MHz, CDCl<sub>3</sub>): 7.52 (1H, d, *J* = 8.4 Hz), 7.06 (1H, s), 6.90 (1H, d, *J* = 8.4 Hz), 6.20 (2H, s), 6.09 (1H, s), 6.00 (1H, bs), 3.87 (3H, s), 3.78 (6H, s), 3.52 (2H, s); <sup>13</sup>CNMR (100 MHz, CDCl<sub>3</sub>): δ 161.6, 158.9, 155.3, 150.7, 145.1, 141.4, 126.2, 120.0, 112.3, 111.8, 111.6, 94.3, 92.6, 55.4, 55.2, 30.4; IR (NaCl) 3003, 2935, 2837, 2360, 1600, 1525, 1488, 1310, 1283, 1254, 1202, 1152, 1066, 1033 cm<sup>-1</sup>; HRMS (ESI, positive) *m/z* calcd. for C<sub>19</sub>H<sub>19</sub>N<sub>3</sub>O<sub>3</sub> [M+H]<sup>+</sup>: 338.1499, found: 338.1495; HPLC purity: 97.0%, retention time: 7.66 min (MeOH:CH<sub>2</sub>Cl<sub>2</sub> = 1:9).

**Methyl 3-((6-methoxy-1,4-dihydroindeno[1,2-*c*]pyrazol-3-yl)amino)benzoate (6m)**

This compound was prepared from 5-methoxy-1-indanone (0.1 g, 0.62 mmol) and methyl 3-isothiocyanatobenzoate (**4d**) (0.119 g, 0.62 mmol) using the procedure described for **6a**. Purification by column chromatography with (Hexane:EtOAc = 2:1 v/v) gave methyl 3-((6-methoxy-1,4-dihydroindeno[1,2-*c*]pyrazol-3-yl)amino)benzoate (**6m**) as a white solid (0.0839 g, 0.25 mmol, 40%). mp: 147-148 °C; <sup>1</sup>H NMR (400 MHz, CDCl<sub>3</sub>): δ 7.64 (1H, s), 7.54 (1H, d, *J* = 7.6 Hz), 7.44 (1H, d, *J* = 8.0 Hz), 7.29 (1H, dd, *J* = 8.0, 8.0 Hz), 7.16 (1H, d, *J* = 8.0 Hz), 7.00 (1H, s), 6.82 (1H, s, *J* = 8.0 Hz), 6.39 (1H, bs), 3.88 (3H, s), 3.28 (3H, s), 3.42 (2H, s); <sup>13</sup>CNMR (100 MHz, CDCl<sub>3</sub>): δ 167.3, 158.9, 154.8, 150.7, 143.3, 141.8, 130.9, 129.1, 125.9, 120.9, 120.1, 120.0,

116.4, 112.2, 111.8, 111.2, 55.4, 52.1, 30.3; IR (NaCl) 3734, 2950, 2360, 1716, 1592, 1540, 1508, 1489, 1472, 1284, 1249, 1107, 1034, 999, 752, 687  $\text{cm}^{-1}$ ; HRMS (ESI, positive)  $m/z$  calcd. for  $\text{C}_{19}\text{H}_{17}\text{N}_3\text{O}_3$   $[\text{M}+\text{H}]^+$ : 336.1343, found: 336.1340; HPLC purity: 98.3%, retention time: 7.72 min (MeOH: $\text{CH}_2\text{Cl}_2$  = 1:9); Anal. Calcd for  $\text{C}_{19}\text{H}_{17}\text{N}_3\text{O}_3$ : C: 68.05, H: 5.11, N: 12.53, O: 14.31, found, C: 67.81, H: 5.15, N: 12.47.

### 3-((6-Methoxy-1,4-dihydroindeno[1,2-c]pyrazol-3-yl)amino)benzoic acid (**6n**)

A mixture of methyl 3-((6-methoxy-1,4-dihydroindeno[1,2-c]pyrazol-3-yl)amino)benzoate (**6m**) (0.084 g, 0.25 mmol) was dissolve in THF (5 mL) and a solution of  $\text{LiOH}\cdot\text{H}_2\text{O}$  (0.021 g, 0.5 mmol) in  $\text{H}_2\text{O}$  (1 mL) was added. The mixture was stirred overnight at room temperature. The reaction was quenched with 1N HCl and the mixture was extracted with EtOAc. The organic layer was washed with water and brine, dried over anhydrous  $\text{Na}_2\text{SO}_4$ , and concentrated. The residue was suspended in  $\text{CH}_2\text{Cl}_2$  and filtrated to give 3-((6-methoxy-1,4-dihydroindeno[1,2-c]pyrazol-3-yl)amino)benzoic acid (**6n**) as a whit solid (0.062g, 0.19 mmol, 76%). mp: 239-240  $^\circ\text{C}$ ;  $^1\text{H}$  NMR (400 MHz,  $\text{CD}_3\text{OD}$ ): 7.65 (1H, s), 7.53 (1H, d,  $J$  = 8.0 Hz), 7.47 (1H, d,  $J$  = 7.6 Hz), 7.27 (1H, dd,  $J$  = 7.6, 8.0 Hz), 7.14 (1H, dd,  $J$  = 2.0, 8.0 Hz), 7.10 (1H, s), 6.91 (1H, dd,  $J$  = 2.0, 8.4 Hz), 3.84 (3H, s), 3.50 (2H, s);  $^{13}\text{C}$  NMR (100 MHz,  $\text{CD}_3\text{OD}$ ):  $\delta$  173.3, 159.2, 155.6, 150.9, 143.5, 141.2, 137.0, 128.2, 126.4, 120.3, 119.4, 117.9, 116.2, 112.1, 111.5, 110.3, 54.5, 29.5; IR (KBr) 3274, 2896, 2833, 1551, 1471, 1391,

1310, 1283, 1245, 1083, 1032  $\text{cm}^{-1}$ ; HRMS (ESI, positive)  $m/z$  calcd. for  $\text{C}_{18}\text{H}_{15}\text{N}_3\text{O}_3$   $[\text{M}+\text{H}]^+$ :

322.1186, found: 322.1182; HPLC purity: 100%, retention time: 8.16 min, (MeOH).

***N*-(3-isobutoxyphenyl)-6-methoxy-1,4-dihydroindeno[1,2-*c*]pyrazol-3-amine (6o)**

This compound was prepared from 5-methoxy-1-indanone (0.094 g, 0.58 mmol) and

1-isobutoxy-3-isothiocyanatobenzene (**4e**) (0.12 g, 0.58 mmol) using the procedure described for **6a**.

Purification by column chromatography with (Hexane:EtOAc = 2:1 v/v) gave

*N*-(3-isobutoxyphenyl)-6-methoxy-1,4-dihydroindeno[1,2-*c*]pyrazol-3-amine (**6o**) as a light yellow

solid (0.113 g, 0.32 mmol, 55%). mp: 76-77 °C;  $^1\text{H}$  NMR (400 MHz,  $\text{CDCl}_3$ ):  $\delta$  7.50 (1H, d,  $J$  = 8.4

Hz), 7.17 (1H, dd,  $J$  = 8.0, 8.4 Hz), 7.04 (1H, s), 6.87 (1H, d,  $J$  = 8.4 Hz), 6.58-6.56 (2H, m), 6.48

(1H, d,  $J$  = 7.6 Hz), 6.07 (1H, bs), 3.86 (3H, s), 3.70 (2H, d,  $J$  = 6.4 Hz), 3.48 (2H, s), 2.21-2.02 (1H,

m), 1.03 (3H, s), 1.00 (3H, s);  $^{13}\text{C}$  NMR (100 MHz,  $\text{CDCl}_3$ ):  $\delta$  160.4, 158.9, 155.3, 150.7, 144.4,

141.6, 129.9, 126.3, 120.1, 112.2, 111.9, 111.4, 108.5, 106.3, 102.4, 74.3, 55.4, 30.4, 28.3, 19.3; IR

(NaCl) 3162, 2957, 2360, 1598, 1524, 1494, 1469, 1394, 1310, 1283, 1247, 1192, 1156, 1082, 1034

$\text{cm}^{-1}$ ; HRMS (ESI, positive)  $m/z$  calcd. for  $\text{C}_{21}\text{H}_{23}\text{N}_3\text{O}_2$   $[\text{M}+\text{H}]^+$ : 350.1863, found: 350.1865; HPLC

purity: 95.7%, retention time: 9.53 min (MeOH: $\text{CH}_2\text{Cl}_2$  = 3:97).

**Cell culture**

The human cervical carcinoma cell line HeLa cells were obtained the Cell Resource Center for Biomedical Research, Institute of Development, Aging and Cancer, Tohoku University (Sendai, Japan). The cells were cultured under 5% CO<sub>2</sub> at 37 °C in RPMI 1640 medium (Wako pure Chemical, Osaka, Japan) supplemented with 10% fetal bovine serum (FBS, HyClone, Logan, UT), 100 U/mL penicillin and 100 µg/mL streptomycin (Invitrogen, Carlsbad, CA). For subsequent experiments, the cells were seeded at a density of 2.5 x 10<sup>5</sup> cells/mL/well in a 12-well TC plate (Greiner Japan, Tokyo, Japan), and incubated at 37 °C for 12h. Hypoxic condition was achieved by replacing cells to 1% O<sub>2</sub>, 95% N<sub>2</sub> and 5% CO<sub>2</sub> in a multigas incubator (Astec, Fukuoka, Japan).

#### MTT assay

HeLa cells were plated on 96 wells plate (5 x 10<sup>3</sup> cells per well ) and incubated at 37 °C for 6 h in 100 µL medium. The cells were incubated for 72h with or without drugs. After incubation, MTT solution in PBS (5 mg/mL) 10 µL was added to each well, and incubated at 37 °C for 2 h. After removal of the supernatant, DMSO 100 µL was added, and the absorbance was determined.

#### Anti-microbial activities

The following microorganisms were used as test strains in the assay; *Staphylococcus aureus* 209 (*S.a.*), *Escherichia coli* HO141 (*E. coli*), *Candida albicans* JCM1542 (*C.a.*), *Aspergillus fumigatus*

Af293 (*A. fumigatus*), and *Magnaporthe oryzae* kita-1 (*M.o.*). Antimicrobial activity of a sample against these microorganisms was examined by a standard microdilution method.

For *S.a.* and *E.c.*, 100  $\mu$ L of inoculum suspension containing 0.1% of a 0.5 McFarland standard suspension was plated into 96-well plate. Test compounds were added to the culture medium, and the plates were incubated at 28°C (*S.a.*) or 37 °C (*E. coli*) for 24 h. For *C.a.* and *A. fumigatus*, 200  $\mu$ L of inoculum suspension containing 0.1% of a 0.5 McFarland standard suspension was seeded into 96-well plate, and incubated at 28 °C for 24 h (*C.a.*) or 48 h (*A. fumigatus*). For *M.o.*, 200  $\mu$ L of cell suspension containing 2% of precultured broth in 96-well plate were incubated at 28 °C for 48 h. The growths of these microorganisms were measured by absorbance at 600 nm (Perkin Elmer).

#### Anti-malarial activities

*Plasmodium falciparum* 3D7 (*P.f.*) were cultured at 37 °C under 5.0% CO<sub>2</sub> in human erythrocytes (3% hematocrit) in RPMI1640 (Invitrogen/Life Technologies), supplemented with 10% human plasma. To perform the *P.f.* growth assay, 100  $\mu$ L of 0.3%-parasitized red blood cells and 2% hematocrit were dispensed into 96-well plate. Following 72-h exposures to test sample, plates were frozen at -70 °C overnight and then thawed at room temperature for at least 4 h. To evaluate LDH activity, 150  $\mu$ L of freshly made reaction mix (166 mM sodium L-lactate, 166  $\mu$ M 3-acetyl pyridine adenine dinucleotide, 208  $\mu$ M Nitro Blue tetrazolium chloride, 150  $\mu$ g/mL diaphorase (22.5 U/mL),

0.8% Tween 20, 116 mM Tris-HCl, pH 8.0) was added. Plates were shaken to ensure mixing and absorbance at 650 nm was monitored in a plate reader (Perkin Elmer) after 10 min of incubation at room temperature.

### Target estimation by MorphoBase profiling

MorphoBase profiling was performed as previously described.<sup>23,24</sup> Briefly, *src<sup>ts</sup>*-NRK and HeLa cells were plated on poly-D-lysine-coated, black, 96-well clear-bottom plates (Bio-one µclear, Greiner). After exposure to compound **6m** (*src<sup>ts</sup>*-NRK; 50 nM, HeLa; 5 nM), the cells were fixed with 3.7% formalin and stained with Hoechst33342 (Sigma-Aldrich). Brightfield images and corresponding nuclear images were acquired on an IN Cell Analyzer 2000 (GE Healthcare). Approximately 1000 cells from these images were analyzed with custom-designed image analysis algorithms to segment individual cells and to measure 12 user-defined descriptors, such as nuclear and cellular area, for each cell. To characterize phenotypic responses at the well level, the average, median, and standard deviation of each parametric measurement was calculated. A total of 71 parameters were normalized to the average corresponding control values of the DMSO-treated cells. Common logarithmic outputs were then applied to the subsequent statistical analysis. For PCA, the eigenvalue-eigenvector of the covariance matrix was calculated, and the resulting principal component scores were displayed in a 2D-scatter plot. The prediction of a target molecule or the mechanism of action of a



test drug was demonstrated by performing two statistical computations: probability scores and the ranking of the nearest neighbors to a test compound determined by Euclidean distance between the compounds.

### Target Estimation by ChemProteoBase Profiling

ChemProteoBase profiling was performed as previously described.<sup>25,26</sup> Briefly, HeLa cells were treated with 2 nM of GN39482 for 18 h. Proteome analysis of cell lysates was performed using a 2-D DIGE system (GE Healthcare), and images of the gels were analyzed using Progenesis SameSpots (Nonlinear Dynamics). Out of more than 1000 spots detectable in each 2DE gel, 296 variational spots that were found in common between gels of reference compound-treated cells were selected as described. Next, the volume of each spot was normalized using the average of the corresponding control values from DMSO-treated HeLa cells. Using the normalized volume of the 296 spots, cosine similarity between compounds was calculated and hierarchical clustering analysis was performed using Gene Cluster 3.0 (clustering method; centroid linkage with the means of uncentered correlation).<sup>31</sup> The predictive dendrogram was visualized using Java Treeview 1.1.3.<sup>32</sup>

### *In vitro* tubulin polymerization assay

*In vitro* tubulin polymerization assay was performed using the Tubulin Polymerization Assay Kit

(Cytoskeleton) per the manufacturer's instructions. Briefly, lyophilized porcine tubulin was solubilized to a final concentration of 2 mg/mL in reaction buffer, containing 80 mM PIPES (pH 6.9), 2 mM MgCl<sub>2</sub>, 0.5 mM EGTA, 1 mM GTP, 10 μM fluorescent reporter, and 20% glycerol, and kept at 4°C. Compounds, (100× DMSO stock solutions) were added to pre-warmed half-area 96-well black plates at 37°C. Cold tubulin solution was added to the wells, the plate contents were mixed by shaking, and the absorbance at 340 nm was read every minute for 1 h.

### Flow Cytometry

Flow cytometry was performed as previously described.<sup>24,26</sup> Briefly, HeLa cells were treated with the designated concentration of compounds for 24 h. Ethanol-fixed cells were washed with PBS and stained in PI buffer (PBS containing 50 μg/mL propidium iodide and 2 μg/mL RNase A (Nacalai Tesque) for 30 min. The DNA content of the cells was analyzed using a Cytomics FC500 (Beckman Coulter).

### Western blotting

After drug treatment for 4h, the cells were washed with PBS (Ca/Mg-free) three times, dipped in 100 μL of ice-cold lysis buffer (20 mM HEPES, pH = 7.4, 1% triton X-100, 10% glycerol, 1 mM EDTA, 5 mM sodium fluoride, 2.5 mM *p*-nitrophenylene phosphate, 10 μg/mL

phenylmethylsulfonylfluoride, 1 mM sodium, and 10  $\mu\text{g/mL}$  leupeptin) for 15 min, and disrupted with a Handy Sonic Disrupter, and the lysate was boiled for 5 min in a sample buffer (50 mM Tris, pH 7.4, 4% SDS, 10% glycerol, 4% 2-thioethanol, and 50  $\mu\text{g/mL}$  bromophenol blue) at a ratio of 4:1. The cell lysates were subjected to SDS-polyacrylamide gel electrophoresis (PAGE), transferred to polyvinylidene difluoride (PVDF) membrane (GE Healthcare Buckinghamshire, UK), and immunoblotted with anti-acetylated  $\alpha$  tubulin antibody (Santa Cruz Biotechnology, Santa Cruz, CA) and anti- $\alpha$  Tubulin antibody (Santa Cruz Biotechnology, Santa Cruz, CA). After further incubation with horseradish peroxidase (HRP)-conjugated secondary antibody, the blot was treated with ECL kit (GE Healthcare) and protein expression was visualized with a Molecular Imager ChemiDoc XRS System (Bio-Rad, Hercules, CA)

### Immunofluorescence

HeLa cells were plated on p35 dishes ( $1 \times 10^4$  cells) containing 1 cm diameter glass coverslips and incubated at 37 °C for 24 h. After drug treatment for 1 h under normoxia, the cells were incubated for 4h under hypoxia. After removing medium, the cells were fixed in 4% paraformaldehyde in PBS for 15 min. After washing with PBS, the cells were permeabilized with 0.4% Triton X-100 in PBS for 5 min, blocked with ImmunoBlock (DS Pharma Biomedical Co. Ltd, Osaka, Japan) for 5 min, and then incubated overnight at 4 °C with anti- $\alpha$  tubulin antibody (Santa Cruz Biotechnology, Santa Cruz,

CA). After washing with PBS, the cells were incubated with FITC-conjugated secondary antibody (Santa Cruz Biotechnology, Santa Cruz, CA) for 2h, and after washing with PBS, treated with 100 nM DAPI (Wako Pure Chemicals, Osaka, Japan) for 5 min. The cells were washed two times with PBS, mounted with ProLong Gold Antifade Reagent (Invitrogen, Carlsbad, CA), and analyzed under an Olympus IX71 fluorescence microscope (Tokyo, Japan).

### Associated Content

#### Supporting Information

*In vitro* kinase inhibition assays of compound **6m** toward EGFR, KDR, PDGFR $\beta$ , CDK2/CycE1, CDK4/CycD3, and CHK1 kinases and chemical structures of compounds with code numbers indicated in Figures 2 and 3. This material is available free of charge via the Internet at <http://pubs.acs.org>.

### Author Information

#### Corresponding author

\*Dr. Hiroyuki Nakamura. Tel.: +81-45-924-5244. E-mail: [hiro@res.titech.ac.jp](mailto:hiro@res.titech.ac.jp).

#### Notes

The authors declare no competing financial interest.

### Abbreviations Used

CDK, cyclin dependent kinase; Chk1, checkpoint kinase 1; EGFR, epidermal growth factor receptor; EPO, erythropoietin; HIF, hypoxia inducible factor; LiHMDS, lithium hexamethyldisilazide; MTT, 3-(4,5-dimethylthiazol-2-yl)-2,5-diphenyltetrazolium bromide; PCA, principal component analysis; PDGFR, platelet-derived growth factor receptor; TBAF, tetrabutylammonium fluoride; VEGFR, vascular endothelial growth factor receptor.

### Acknowledgments

This work was partially supported by a Grant-in-Aid for Scientific Research on Innovative Areas “Chemical Biology of Natural Products” from The Ministry of Education, Culture, Sports, Science and Technology, Japan. We thank Harumi Aono (RIKEN), Yasuko Hirata (RIKEN), Naoko Morita (RIKEN), and Hiroki Hayase (RIKEN) for technical assistance. H. Minegishi gratefully acknowledges the financial support by the Japan Society for the Promotion of Science (JSPS, ID No. 2611488).

### References

[1] Boyd, G. V. Pseudoazulenes containing 2 fused 5-membered rings. *Tetrahedron Lett.*, **1965**, 6,

1  
2  
3  
4  
5  
6 1421-1426.  
7  
8

9 [2] Lemke, T. L.; Cramer, M. B.; Shanmugam, K. Heterocyclic tricycles as potential CNS agents .1.  
10  
11 - 4-aminoalkylindeno[1,2-c]pyrazoles. *J. Pharm. Sci.*, **1978**, *67*, 1377-1381.  
12  
13

14 [3] Albertini, S.; Bos, M.; Gocke, E.; Kirchner, S.; Muster, W.; Wichmann, J.; Suppression of  
15  
16 mutagenic activity of a series of 5HT2c receptor agonists by the incorporation of a gem-dimethyl  
17  
18 group: SAR using the ames test and a DNA unwinding assay. *Mutagenesis*, **1998**, *13*, 397-403.  
19  
20

21 [4] Nugiel, D. A.; Vidwans. A.; Etzkorn, A-M.; Rossi, K. A.; Benfield, P. A.; Burton, C. R.; Cox, S.;  
22  
23 Doleniak, D.; Seitz, S. P. Synthesis and evaluation of indenopyrazoles as cyclin-dependent kinase  
24  
25 inhibitors. 2. Probing the indeno ring substituent pattern. *J. Med. Chem.* **2002**, *45*, 5224-5232.  
26  
27  
28

29 [5] Yue, E. W.; Higley. C. A.; DiMeo, S. V.; Carini, D. J.; Nugiel, D. A.; Benware, C.; Benfield, P.  
30  
31 A.; Burton, C. R.; Cox, S.; Grafstrom, R. H.; Sharp, D. M.; Sisk, L. M.; Boylan, J. F.; Muckelbauer,  
32  
33 J. K.; Smallwood, A. M.; Chen, H.; Chang, C-H.; Seitz. S. P.; Trainor, G. L. Synthesis and evaluation  
34  
35 of indenopyrazoles as cyclin-dependent kinase inhibitors. 3. Structure activity relationships at C3. *J.*  
36  
37 *Med. Chem.* **2002**, *45*, 5233-5248.  
38  
39  
40  
41  
42  
43  
44

45 [6] Ho, C. Y.; Ludovici, D. W.; Maharroof, U. S. M.; Mei, J.; Sechler, J. L.; Tuman, R. W.; Strobel, E.  
46  
47 D.; Andraka, L.; Yen, H.-K.; Leo, G.; Li, J.; Almond, H.; Lu, H.; DeVine, A.; Tominovich, R. M.;  
48  
49 Baker, J.; Emanuel, S.; Gruninger, R. H.; Middleton, S. A.; Johnson, D. L.; Galemno, R. A.  
50  
51  
52  
53  
54  
55  
56 (6,7-Dimethoxy-2,4-dihydroindeno[1,2-c]pyrazol-3-yl)phenylamines: Platelet-derived growth factor  
57  
58  
59  
60

receptor tyrosine kinase inhibitors with broad antiproliferative activity against tumor cells. *J. Med.*

*Chem.* **2005**, *48*, 8163–8173.

[7] Tao, Z-F.; Li, G.; Tong, Y.; Chen, Z.; Merta, P.; Kovar, P.; Zhang, H.; Rosenberg, S-H.; Sham, H.

L.; Sowin, T. J.; Lin, N-H. Synthesis and biological evaluation of

4'-(6,7-disubstituted-2,4-dihydro-indeno[1,2-c]pyrazol-3-yl)-biphenyl-4-ol as potent Chk1 inhibitors.

*Bioorg. Med. Chem. Lett.* **2007**, *17*, 4308-4315.

[8] Tao, Z-F.; Li, G.; Tong, Y.; Stewart, K. D.; Chen, Z.; Bui, M-H.; Merta, P.; Park, C.; Kovar, P.;

Zhang, H.; Sham, H. L.; Rosenberg, S. H.; Sowin, T. J.; Lin, N-H. Discovery of

4'-(1,4-dihydro-indeno[1,2-c]pyrazol-3-yl)-benzonitriles and

4'-(1,4-dihydro-indeno[1,2-c]pyrazol-3-yl)-pyridine-2'-carbonitriles as potent checkpointkinase 1

(Chk1) inhibitors. *Bioorg. Med. Chem. Lett.* **2007**, *17*, 5944-5951.

[9] Usui, T.; Ban, H. S.; Kawada, J.; Hirokawa, T.; Nakamura, H. Discovery of indenopyrazoles as

EGFR and VEGFR-2 tyrosine kinase inhibitors by in silico high-throughput screening. *Bioorg. Med.*

*Chem. Lett.* **2008**, *18*, 285-288.

[10] Saghaie, L.; Shahlaei, M.; Madadkar-Sobhani, A.; Fassihi, A. Application of partial least

squares and radial basis function neural networks in multivariate imaging analysis-quantitative

structure activity relationship: study of cyclin dependent kinase 4 inhibitors. *J. Mol. Graph. Model.*

**2010**, *29*, 518-528.

- [11] Wang, G. L.; Jiang, B. H.; Rue, E. A.; Semenza, G. L. Hypoxia-inducible factor 1 is a basic-helix-loop-helix-PAS heterodimer regulated by cellular O<sub>2</sub> tension. *Proc. Natl. Acad. Sci. USA*, **1995**, *92*, 5510-5514.
- [12] Wang, G. L.; Semenza, G. L. Purification and characterization of hypoxia-inducible factor 1. *J. Biol. Chem.* **1995**, *270*, 1230-1237.
- [13] Ferrara, N.; Gerber, H. P.; LeCouter, J. The biology of VEGF and its receptors. *Nat. Med.* **2003**, *9*, 669-676.
- [14] Jaakkola, P.; Mole, D. R.; Tian, Y. M.; Wilson, M. I.; Gielbert, J.; Gaskell, S. J.; von Kriegsheim, A.; Hebestreit, H. F.; Mukherji, M.; Schofield, C. J.; Maxwell, P. H.; Pugh, C. W.; Ratcliffe, P. J. Targeting of HIF- $\alpha$  to the von Hippel-Lindau ubiquitylation complex by O<sub>2</sub>-regulated prolyl hydroxylation. *Science*. **2001**, *292*, 468-472.
- [15] Ivan, M.; Kondo, K.; Yang, H.; Kim, W.; Valiando, J.; Ohh, M.; Salic, A.; Asara, J. M.; Lane, W. S.; Kaelin, W. G. Jr. HIF $\alpha$  targeted for VHL-mediated destruction by proline hydroxylation: implications for O<sub>2</sub> sensing. *Science*. **2001**, *292*, 464-468.
- [16] Talks, K. L.; Turley, H.; Gatter, K. C.; Maxwell, P. H.; Pugh, C. W.; Ratcliffe, P. J.; Harris, A. L. The expression and distribution of the hypoxia-inducible factors HIF-1 $\alpha$  and HIF-2 $\alpha$  in normal human tissues, cancers, and tumor-associated macrophages. *Am. J. Pathol.*, **2000**, *157*, 411-421.
- [17] Birner, P.; Schindl, M.; Obermair, A.; Breitenecker, G.; Oberhuber, G. Expression of



hypoxia-inducible factor 1 $\alpha$  in epithelial ovarian tumors: Its impact on prognosis and on response to chemotherapy. *Clin. Cancer. Res.*, **2001**, 7, 1661-1668.

[18] Birner, P.; Gatterbauer, B.; Oberhuber, G.; Schindl, M.; Rössler, K.; Proding, A.; Budka, H.; Hainfellner, J. A. Expression of hypoxia-inducible factor-1 $\alpha$  in oligodendrogliomas : Its impact on prognosis and on neoangiogenesis. *Cancer*, **2001**, 92, 165-171.

[19] Giatromanolaki, A.; Koukourakis, M. I.; Sivridis, E.; Turley, H.; Talks, K.; Pezzella, F.; Gatter, K. C.; Harris, A. L. Relation of hypoxia inducible factor 1 $\alpha$  and 2 $\alpha$  in operable non-small cell lung cancer to angiogenic/molecular profile of tumours and survival. *Br. J. Cancer*, **2001**, 85, 881-890.

[20] Zagzag, D.; Zhong, H.; Scalzitti, J. M.; Laughner, E.; Simons, J. W.; Semenza, G. L. Expression of hypoxia-inducible factor 1 $\alpha$  in brain tumors : Association with angiogenesis, invasion, and progression. *Cancer*, **2000**, 88, 2606-2618.

[21] Birner, P.; Schindl, M.; Obermair, A.; Plank, C.; Breiteneker, G.; Oberhuber, G. Overexpression of hypoxia-inducible factor 1 $\alpha$  is a marker for an unfavorable prognosis in early-stage invasive cervical cancer. *Cancer Res.* **2000**, 60, 4693-4696.

[22] Minegishi, H.; Fukushima, S.; Ban, H. S.; Nakamura, H. Discovery of indenopyrazoles as new class of hypoxia inducible factor (HIF)-1 inhibitor. *ACS. Med. Chem. Lett.* **2013**, 4, 297-301

[23] Futamura, Y.; Kawatani, M.; Kazami, S.; Tanaka, K.; Muroi, M.; Shimizu, T.; Tomita, K.; Watanabe, N.; Osada, H. MorphoBase, an encyclopedic cell morphology database, and its use for

drug target identification. *Chem. Biol.* **2012**, *19*, 1620-1630.

[24] Muroi, M.; Kazami, S.; Noda, K.; Kondo, H.; Takayama, H.; Kawatani, M.; Usui, T.; Osada, H.

Application of proteomic profiling based on 2D-DIGE for classification of compounds according to the mechanism of action. *Chem. Biol.* **2010**, *17*, 460-470.

[25] Kawatani, M.; Takayama, M.; Muroi, M.; Kimura, S.; Maekawa, T.; Osada, H. Identification of a small-molecule inhibitor of DNA topoisomerase II by proteomic profiling. *Chem. Biol.* **2011**, *18*, 743-751.

[26] Futamura, Y.; Kawatani, M.; Muroi, M.; Aono, H.; Nogawa, T.; Osada, H. Identification of a molecular target of a novel fungal metabolite, pyrrolizilactone, by phenotypic profiling systems. *ChemBioChem.* **2013**, *14*, 2456-2463.

[27] Zhang, X.; Lee, Y.K.; Kelley, J. A.; Burke, T. R. Preparation of aryl isothiocyanates via protected phenylthiocarbamates and application to the synthesis of caffeic acid (4-isothiocyanato)phenyl ester. *J. Org. Chem.* **2000**, *65*, 6237-6240

[28] Ahsan, M. J.; Samy, J. G.; Soni, S.; Jain, N.; Kumar, L.; Sharma, L. K.; Yadav, H.; Saini, L.; Kalyansing, R. G.; Devenda, N. S.; Prasad, R.; Jain, C. B. Discovery of novel antitubercular 3a,4-dihydro-3H-indeno[1,2-c]pyrazole-2-carboxamide/carbothioamide analogues. *Bioorg Med Chem Lett.* **2011**, *21*, 5259-5261.

[29] Ahsan, M. J.; Samy, J. G.; Khalilullah, H.; Bakht, M. A.; Hassan, M. Z. Synthesis and

antimycobacterial evaluation of 3a,4-dihydro-3H-indeno [1,2-c] pyrazole-2-carboxamide analogues.

*Eur. J. Med. Chem.* **2011**, *46*, 5694-5697.

[30] Mollinedo, F.; Gajate, C. Microtubules, microtubule-interfering agents and apoptosis. *Apoptosis*.

**2003**, *8*, 413-450.

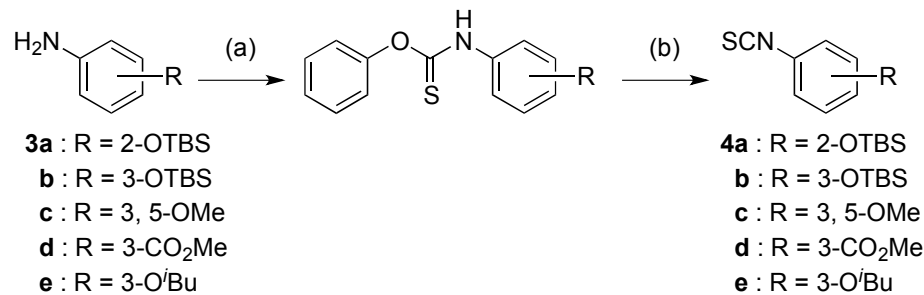
[31] de Hoon, M. J.; Imoto, S.; Nolan, J.; Miyano, S. Open source clustering software.

*Bioinformatics*. **2004**, *20*, 1453-1454

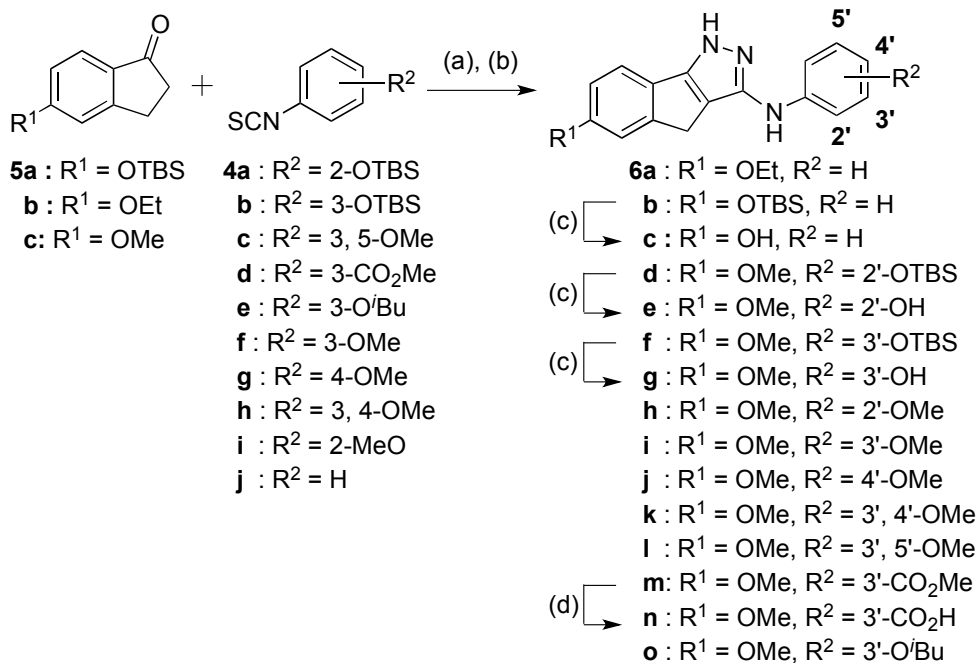
[32] Saldanha, A. J. Java treeview-extensible visualization of microarray data. *Bioinformatics*. **2004**,

*20*, 3246-3248

**Scheme 1.** Synthesis of phenyl isothiocyanates **4a-e**



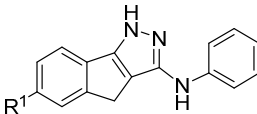
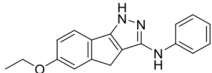
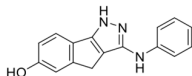
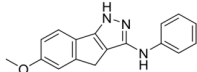
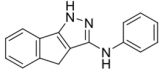
*Reagents and conditions:* (a) Phenyl chlorothionoformate, THF. (b) TEA, Cl<sub>3</sub>SiH, toluene, 96->99%

**Scheme 2.** Synthesis of indenopyrazoles **6a-o**

*Reagents and conditions:* (a) LiHMDS, THF, 12 h. (b) H<sub>2</sub>NNH<sub>2</sub>·H<sub>2</sub>O, AcOH, reflux, 24 h, 37-60%,

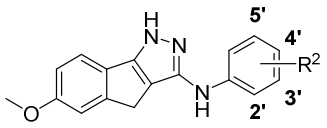
(c) TBAF, THF, 47%-quant. (d) LiOH·H<sub>2</sub>O, THF, H<sub>2</sub>O, 76%

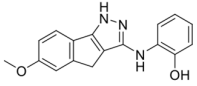
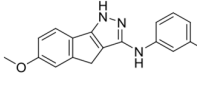
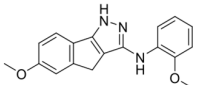
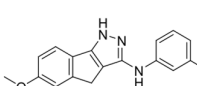
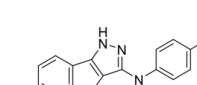
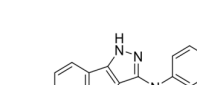

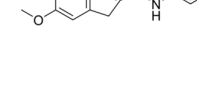
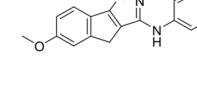
PC3, HCT116, and HEK293 cells

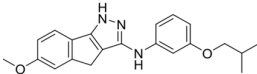
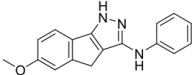
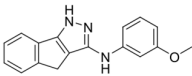
					
compd		IC <sub>50</sub> (nM) 72h			
		HeLa	PC3	HCT116	HEK293
	<b>6a</b>	20.4 ± 1.19	60.2 ± 12.7	56.8 ± 5.2	55.6 ± 3.4
	<b>6c</b>	>100	>100	>100	>100
	<b>2</b> <sup>19</sup>	8.9 ± 0.37	35.6 ± 4.8	26.6 ± 1.4	53.6 ± 18.6
	<b>6p</b> <sup>19</sup>	>100	>100	>100	>100

Cells were incubated with various concentrations (0.3–100 nM) of compounds for 72 h, and cell viability was determined by the MTT assay.

**Table 2.** Substituent effects at R<sup>2</sup> position of 6-methoxy-substituted indenopyrazoles on proliferative activity toward HeLa, PC3, HCT116, and HEK293 cells

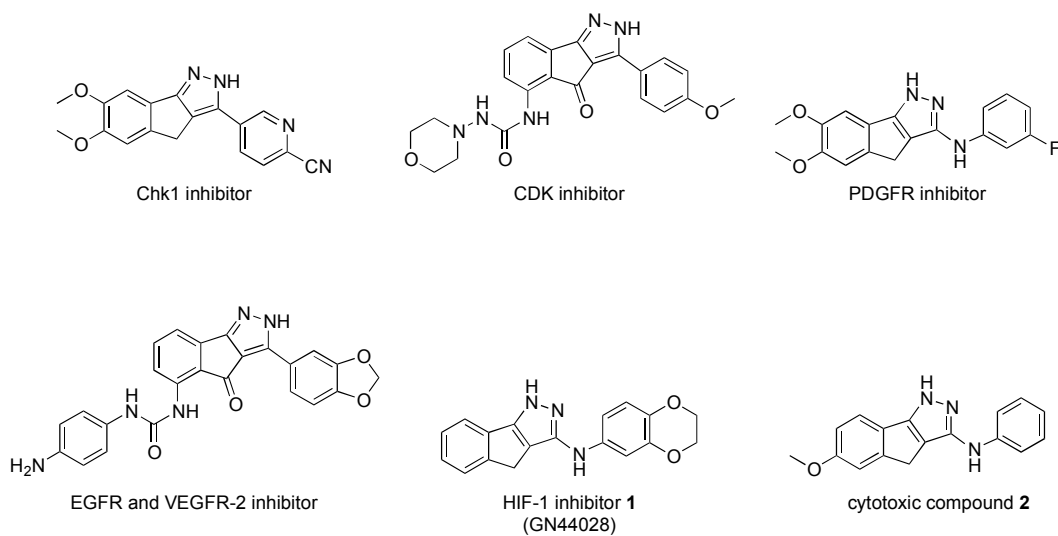


compd	IC <sub>50</sub> (nM) 72h			
	HeLa	PC3	HCT116	HEK293
	<b>6e</b>	>100	>100	>100
	<b>6g</b>	7.1 ± 0.15	8.6 ± 1.2	10.9 ± 0.9
	<b>6h</b>	32.0 ± 1.21	>100	86.2 ± 10.4
	<b>6i</b>	2.8 ± 0.16	4.7 ± 0.5	6.53 ± 0.96
	<b>6j</b>	>100	>100	>100
	<b>6k</b>	>100	90.9 ± 3.8	86.3 ± 5.4
	<b>6l</b>	3.20 ± 0.05	7.0 ± 1.1	7.4 ± 0.6
	<b>6m</b> (GN39482)	2.47 ± 0.07	2.64 ± 0.07	2.7 ± 0.2
	<b>6n</b>	>100	>100	>100

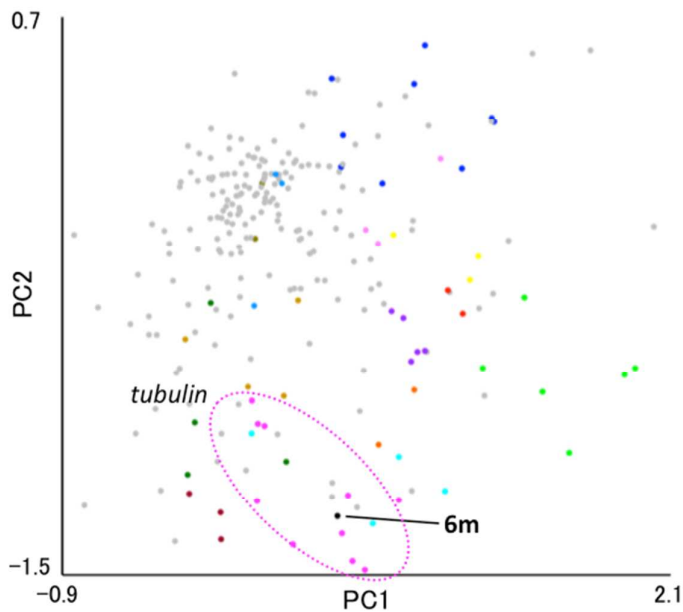
	<b>6o</b>	$19.95 \pm 1.01$	$50.5 \pm 7.4$	$56.6 \pm 1.6$	$25.5 \pm 1.0$
	<b>2<sup>19</sup></b>	$8.9 \pm 0.37$	$35.6 \pm 4.8$	$26.6 \pm 1.4$	$53.6 \pm 18.6$
	<b>6q<sup>19</sup></b>	$>100$	$>100$	$>100$	$>100$

Cells were incubated with various concentrations (0.3–100 nM) of compounds for 72 h, and cell viability was determined by the MTT assay.





**Figure 1.** Structures of biologically active indenopyrazoles



Probability score			Similarity ranking					
Rank	Class	Score	Rank	Sample	Class	Target	MOA	Distance
1	tubulin	1.68	1	rotenone		complex I, tubulin	mitochondria respiration	0.97
2	Eg5	2.39	2	paspaline	Eg5	Eg5	microtubule dynamics	0.97
3	DNA	2.69	3	SB225002		CXCR2	chemokine receptor	0.98
4	ionophore	3.17	4	NPD8617	tubulin	tubulin	microtubule dynamics	1.00
5	V-ATPase	3.53	5	NPD6689	tubulin	tubulin	microtubule dynamics	1.03
6	proteasome	3.56	6	vinblastine	tubulin	tubulin	microtubule dynamics	1.07
7	actin	3.78	7	NPD8969	tubulin	tubulin	microtubule dynamics	1.07
8	HSP60	3.85	8	manumycin A		FTase/GGTase	second messenger	1.08
9	PP2A	4.27	9	GN26361	HSP60	HSP60	heat shock protein	1.09
10	RNA	4.51	10	toutomycin	PP2A	PP1/PP2A	phosphatase	1.12
11	HSP90	5.18	11	noscapine	tubulin	tubulin	microtubule dynamics	1.13
12	protein	6.00	12	ETB	HSP60	HSP60	heat shock protein	1.14
13	control	6.07	13	terpendole E	Eg5	Eg5	microtubule dynamics	1.14
14	HDAC	6.68	14	concanamycin A	V-ATPase	V-ATPase	vesicle trafficking	1.14
15	TOP2 cat	8.85	15	nocodazole	tubulin	tubulin	microtubule dynamics	1.15

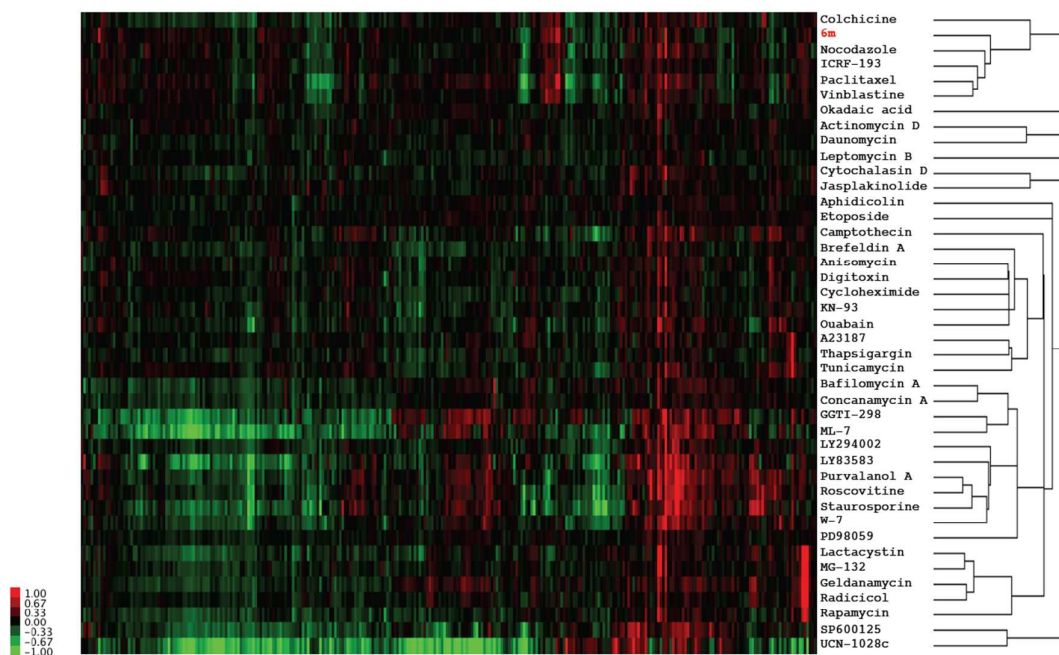
**Figure 2.** Target protein profilings of compound **6m** analyzed by MorphoBase. Chemical structures of compounds with code numbers are indicated in the Supporting Information.

Top 10 compounds similar to **6m**

Ranking	Cosine similarity	Compound	Target of compound
1	0.74	Vinblastine	tubulin
2	0.71	Paclitaxel	tubulin
3	0.7	NPD6689	tubulin
4	0.68	BNS-22	Topo II (catalytic)
5	0.66	NPD8617	tubulin
6	0.66	ICRF-193	Topo II (catalytic)
7	0.64	Rotenone	tubulin, respiration
8	0.63	BI 2536	PLK-1
9	0.63	NPD8969	tubulin
10	0.61	Monastrol	Eg5

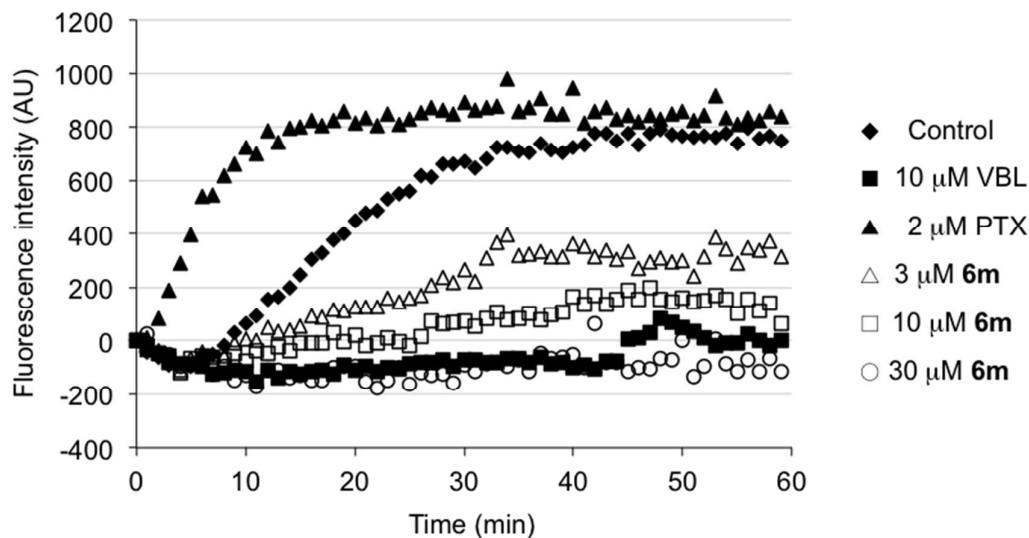
## Histogram of compounds

0.9~1.0 :  
 0.8~ :  
 0.7~ : \*\*\*  
 0.6~ : \*\*\*\*\*  
 0.5~ : \*\*  
 0.4~ : \*  
 0.3~ : \*\*\*\*\*  
 0.2~ : \*\*\*\*\*  
 0.1~ : \*\*\*\*\*  
 0.0~ : \*\*\*\*\*  
 -0.1~ : \*\*\*\*\*  
 -0.2~ : \*\*\*\*\*  
 -0.3~ : \*\*  
 -0.4~ :

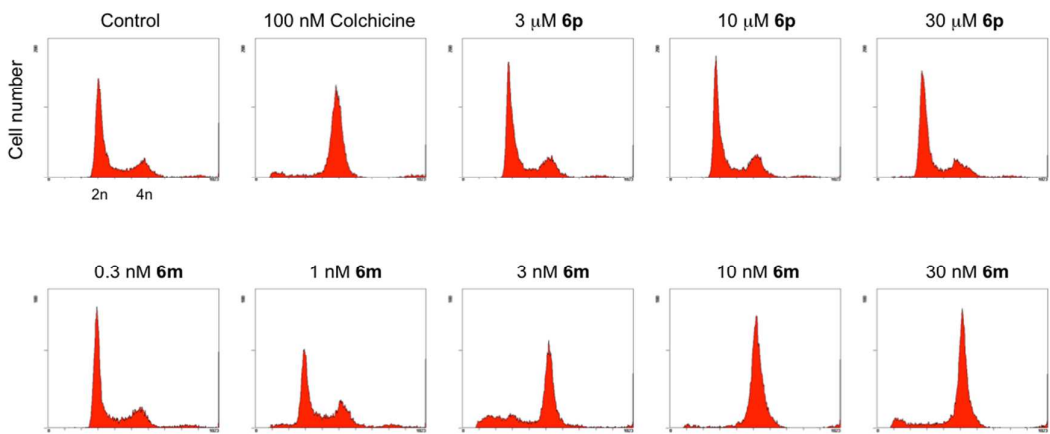


**Figure 3.** Clustering of well-characterized compounds and compound **6m** by proteomic analysis of HeLa cells. Chemical structures of compounds with code numbers are indicated in the Supporting Information.

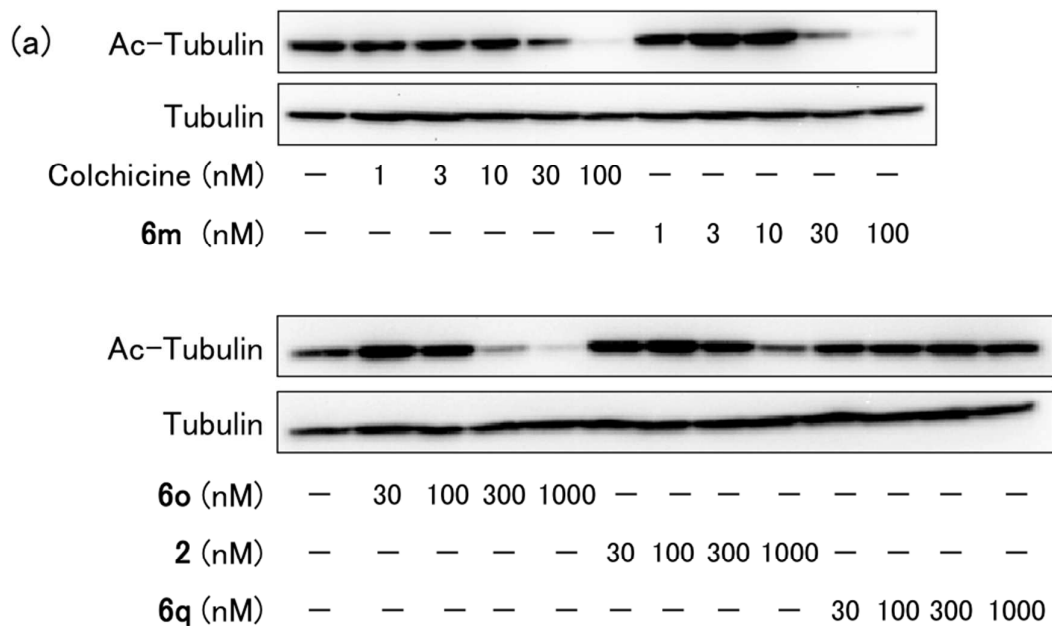
1  
2  
3  
4  
5  
6  
7  
8  
9  
10  
11  
12  
13  
14  
15  
16  
17  
18  
19  
20  
21  
22  
23  
24  
25  
26  
27  
28  
29  
30  
31  
32  
33  
34  
35  
36  
37  
38  
39  
40  
41  
42  
43  
44  
45  
46  
47  
48  
49  
50  
51  
52  
53  
54  
55  
56  
57  
58  
59  
60



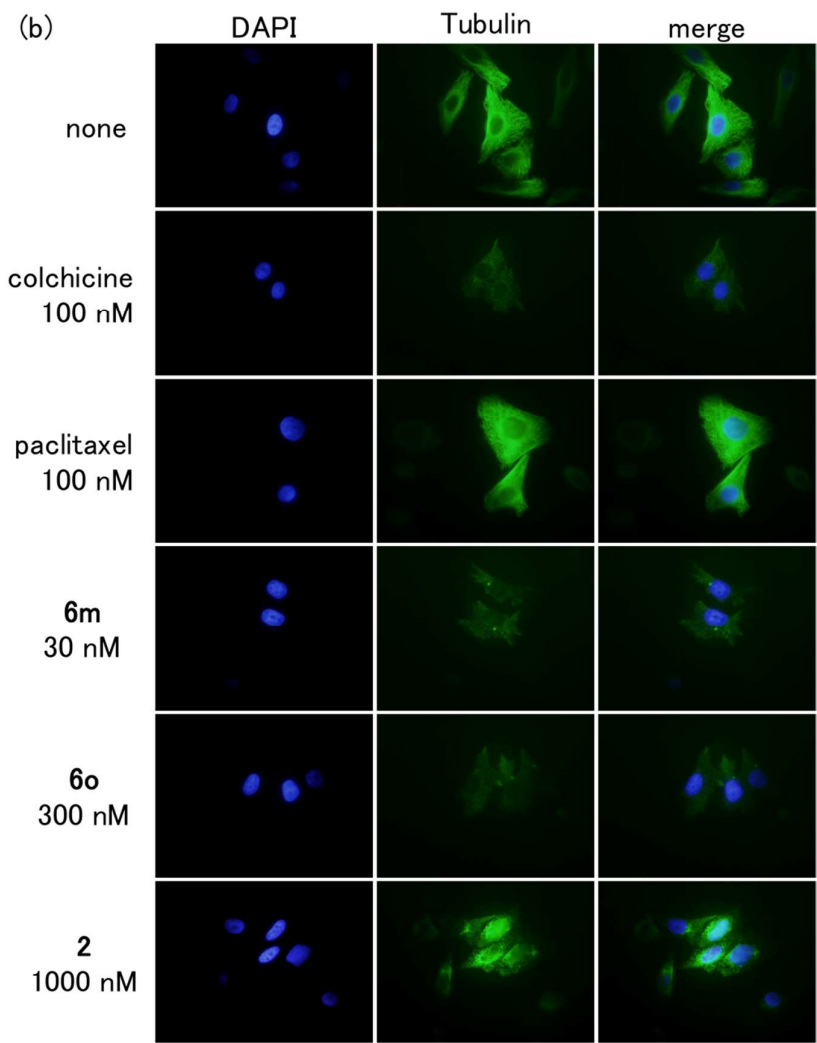
**Figure 4.** Concentration-dependent inhibition of tubulin formation by **6m**. Lyophilized porcine tubulin was solubilized to a final concentration of 2 mg/mL in reaction buffer, containing 80 mM PIPES (pH 6.9), 2 mM  $\text{MgCl}_2$ , 0.5 mM EGTA, 1 mM GTP, 10  $\mu$ M fluorescent reporter, and 20% glycerol, and kept at 4°C. Compounds, (100 $\times$  DMSO stock solutions) were added to pre-warmed half-area 96-well black plates at 37°C. Cold tubulin solution was added to the wells, the plate contents were mixed by shaking, and the absorbance at 340 nm was read every minute for 1 h. Vinblastine (VBL) and Paclitaxel (PTX) were used as positive and negative controls, respectively.



**Figure 5.** Effects of compound **6m** on cell cycles of HeLa cells. The cells were treated with compounds for 24 h. Ethanol-fixed cells were washed with PBS and stained in PI buffer (PBS containing 50 μg/mL propidium iodide and 2 μg/mL RNase A (Nacalai Tesque) for 30 min. The DNA content of the cells was analyzed using a flow cytometry. Colchicine and compound **6p** were used as positive and negative controls, respectively.



1  
2  
3  
4  
5  
6  
7  
8  
9  
10  
11  
12  
13  
14  
15  
16  
17  
18  
19  
20  
21  
22  
23  
24  
25  
26  
27  
28  
29  
30  
31  
32  
33  
34  
35  
36  
37  
38  
39  
40  
41  
42  
43  
44  
45  
46  
47  
48  
49  
50  
51  
52  
53  
54  
55  
56  
57  
58  
59  
60



**Figure 6.** Effects of indenopyrazoles on tubulin polymerization and microtubule dynamics

HeLa cells were incubated for 6 h with or without compounds. (a) Tubulin and acetylated tubulin (Ac-tubulin) protein expression was detected by immunoblot analysis with the specific antibody. Colchicine was used as a positive control for the inhibition of Ac-tubulin accumulation. (b) Microtubule was detected by immunofluorescence with the specific tubulin antibody. Nuclei were visualized by staining with DAPI.



## TOC Graphic

